IMPLEMENTATION AND EXPERIMENTAL CHARACTERIZATION OF A NOVEL, FUEL-FLEXIBLE, LABORATORYSCALE, PREMIXED COMBUSTOR FOR PREHEATED GAS

By

JULIEN BRISSONNEAU

A THESIS PRESENTED TO THE GRADUATE SCHOOL
OF THE UNIVERSITY OF FLORIDA IN PARTIAL FULFILLMENT
OF THE REQUIREMENTS FOR THE DEGREE OF
MASTER OF SCIENCE

UNIVERSITY OF FLORIDA

2012

© 2012 Julien Brissonneau

To my Grand Dad

ACKNOWLEDGMENTS

I am extremely thankful to Dr. David W. Hahn, Chairman and Knox T. Millsaps Professor at the Department of Mechanical and Aerospace engineering of University of Florida for his whole advisement during my studies. He has very frequently proved his considerable pedagogic skills, scientific knowledge and natural curiosity. Dr. Hahn always took the time to provide me the support I needed to work in the best conditions. I acknowledge my sincere thanks to Dr. William Lear and Dr. David Mikolaitis for serving as members in my committee.

I am very thankful to Benoit Fond, UF alumnus. His good advice and support were very relevant for my project of studies in Florida. I am also graceful to my current and former labmates: Julia, Nathan, Michael, Richard, Sarah, Phil and Kris. They composed a very agreeable team to work with. Our laboratory is definitely a great place for work as well as for discussion and exchange of points of view. Finally, I would like to thank my family for encouraging me to pursue my academic ambitions.

TABLE OF CONTENTS

page

ACKNOWLEDGMENTS 4

TABLE OF CONTENTS 5

LIST OF TABLES 7

LIST OF FIGURES 8

LIST OF ABBREVIATIONS 10

ABSTRACT 12

CHAPTER

1 INTRODUCTION 14

Economical, Fiscal and Geo-Political Implications 14
Nitric Oxides Reduction 16
Synthetic Gas and Fuel-Flexibility 21
Well Stirred Reactor 26

2 STATEMENT OF SCOPE 28

Burner Specific Geometry 28
Operating System Design 34

3 IMPLEMENTATION 35

The Outside Air Supply Subsystem 36
The Inside Air Supply Subsystem 38
The Gas Supply Subsystem 45
The Computer Interface 45
The Liquid Fuel Supply Subsystem 47
The Thermocouples 48
The Gas Analyzer 48

4 EXPERIMENTAL CHARACTERIZATION 50

Starting Procedure 50
Lean Blowout Limit 50
Rich Blowout Limit 52
Nitric Oxides Emissions 52

5 DIFFERENCES BETWEEN MODELS AND EXPERIMENTAL RESULTS 56

Reaction Rate 56
Inlet and Reactor Temperature 57
Experimental Feedback 61

6 FUTURE WORK 63

APPENDIX

A RELEVANT MACHINING DRAWING 66

B BIG PICTURE OF THE SUPPLY SYSTEM 70

LIST OF REFERENCES 72

BIOGRAPHICAL SKETCH 74

LIST OF TABLES

Table		page
0-1	Stoichiometry definitions	11
3-1	List of product for the compressed air supply outside the building	39
3-2	List of flow controllers for the Air and Gas supply	41
3-3	List of product for the air pre-heating system	44
3-4	List of material used for liquid fuel	47

LIST OF FIGURES

Figure		page
1-1	NOx-reducing by exhaust gas recirculation	17
1-2	Schematic stable flame	17
1-3	Schematic unstable flame	18
1-4	Transition from stable to unstable flame due to changes in flow conditions [5]	19
1-5	Burner assembly damaged by combustion instability and new burner assembly [6]	20
1-6	Schematic flameless oxidation	20
1-7	Single flow passage computational grid for a high-speed centrifugal compressor (dim 141x49x33 in the streamwise, spanwise and pitchwise directions) [8]	22
1-8	Calculated and experimental performance map of a a high-speed centrifugal compressor	23
2-1	Dependence of H, OH,C3H3,C2H2, benzene and naphthalene concentrations on equivalence ratio for ethylene combustion (1650K, 1 atm)	29
2-2	A schematic illustration of soot formation according to the ionic theory [17]	30
2-3	Normal cut of B. Fond’s burner	31
2-4	Cuts of B. Fond's combustion chamber	32
2-5	Axial Cut of the combustion chamber	33
3-1	Picture of the annular combustion chamber from the top	35
3-2	Picture of the burner assembly	36
3-3	Pressure evolution in the tank at 35 SCFM	40
3-4	Picture of the outside air supply system	40
3-5	Picture of the flow controllers	42
3-6	Picture of the flow controllers	43
3-7	Picture of the control box operational	44

3-8 Gas supply flexible implementation 46
3-9 Labview interface 47
3-10 Liquid fuel supply subsystem 48
3-11 Gas analyzer 49
4-1 Graphic of the Lean Limit experimentation 51
4-2 Table of the Lean Limit experimentation 51
4-3 Graphic of the Lean Limit experimentation 53
4-4 Table of the Rich Limit experimentation 53
4-5 NOx Measurements 54
4-6 NOx Measurements Graphics 55
5-1 Adiabatic flame temperature for mixtures of CH4/O2/N2 58
5-2 Composition at equilibrium for different methane-air mixtures at initial temperature of 400K and a constant pressure of 1 atmosphere 59
5-3 Schematic representation of the 3 flows and the 3 tubes of the burner's thermal modelisation 61

LIST OF ABBREVIATIONS

P	Density (kg.m3)
M	Dynamic viscosity (Pa.s-1)
Φ	Equivalence ratio
G	Gas (subscript)
Q	Heat (J)
Г	Heat capacity ratio
I	Inlet (subscript)
L	Liquid (subscript)
M	Mach number
$\dot{m}$	Mass flow rate (kg.s-1)
NOX	Nitrogen oxides
PAH	Polycyclic aromatic hydrocarbons
P	Pressure (Pa)
A	Section (m2)
*	Sonic condition (subscript)
q_p	Source term (measured in dBA)
CP	Specific heat at constant pressure (J.kg-1.K)
T	Temperature (K)
K	Thermal conductivity (W.m-1.K-1)
R	Universal gas constant (8.314 J.K-1.mol-1)
U	Velocity(m.s-1)
V	Volume (m3)
W	Wall (subscript)

The following definitions may become useful when reading the text.

Table 0-1. Stoichiometry definitions

Name	Definition	Oxygen requirement	Combustion products
Conventional equivalence ratio	$\Phi_C = \left(\frac{X_F}{X_{O2}}\right) Z_\Phi$	$Z_\Phi = n_C + {}^{n_H}/_4$	CO_2, H_2O
Effective equivalence ratio	$\Psi_C = \left(\frac{X_F}{X_{O2}}\right) Z_\Psi$	$Z_\Psi = {}^{n_C}/_2 + {}^{n_H}/_4$	CO, H_2O
Carbon-to-oxygen ratio	$\left({}^{C}/_{O}\right)_c = \left(\frac{X_F}{X_{O2}}\right) Z_{(C/O)}$	$Z_{(C/O)} = {}^{n_C}/_2$	CO, H_2

Abstract of Thesis Presented to the Graduate School
of the University of Florida in Partial Fulfillment of the
Requirements for the Degree of Master of Science

IMPLEMENTATION AND EXPERIMENTAL CHARACTERIZATION OF A NOVEL, FUEL-FLEXIBLE, LABORATORYSCALE, PREMIXED COMBUSTOR FOR PREHEATED GAS

By

Julien Brissonneau

August 2012

Chair: David W. Hahn
Major: Aerospace Engineering

The challenging, clean, plentiful and full of promise biomass energy sector motivates a global awareness in burning greatly variable fuels in gas turbine combustors. Existing combustor stability and low emission burner technologies are designed for a given fuel composition. The current study aims at implementing a fuel flexible combustion system which can be used for kinetic investigations, as well as for low purity fuels combustion.

A premixed burner previously designed based on the concept of a forced recirculation by jet impingement and strong stirring [1] has been implemented and calibrated. A numerical investigation of the combustion performance had been previously performed on a fully detailed model to define an operative range of interest. The entire system had been designed to provide this range of operation based on detailed heat transfer cooling and gas dynamics injector models. This operative range has been observed with an experimental approach and differences between the previous model and the experimental observations have been quantified, analyzed and explained.

Optical and physical diagnostics capabilities have been implemented in order to provide insight into the reactor chemistry. This allows the characterization of the combustor performance. The research documented in this current paper is part of a larger research effort to investigate kinetics of alternative fuel combustion on the one hand, and of the kinetic effects of CO_2 and H_2O in flameless combustion on the other hand. The long term goal of such investigations is to create a variable geometry combustor with optimized operating configurations allowing perfectly stable flameless combustion for a range of variable fuel compositions. The operating principles are expected to be relevant to the design of conventional gas turbine combustors, as well as the combustion system of novel semi-closed cycle engines.

CHAPTER 1
INTRODUCTION

Economical, Fiscal and Geo-Political Implications

In order to reduce the cost of electricity in today's challenging market environment and to reduce the pollutant emissions, superior efficiency and low ratio of pollutant emission over power generation are one of the key drivers in gas turbine development. In a future resource-constrained world, where public opinions are aware of ecological concerns, environmental taxes are expected to become increasingly important. The financial cost of pollution could take diverse forms such as the carbon tax. It is an environmental tax levied on the carbon content of fuels, a form of carbon pricing. A lot of European countries have already implemented such taxes or, more generally, energy taxes. Most environmentally related taxes with implications for greenhouse gas emissions in OECD (Organization for Economic Co-operation and Development) countries are levied on energy products and motor vehicles, rather than on CO2 emissions directly. In 2010, the European Commission considered implementing a pan-European minimum tax on pollution permits purchased under the EU ETS (European Union Greenhouse Gas Emissions Trading System) in which the proposed new tax would be calculated in terms of carbon content rather than volume, so that fuels with high energy concentrations, despite their subsequently high carbon content, will no longer carry the same traditionally low price. These types of environmentally friendly taxes financially motivate gas turbine efficiency improvements for aircraft propulsion systems. In the United States, Cap and trade is an environmental policy tool based on emission trading that is in force. This is a market-based approach used to control pollution by providing economic incentives for achieving reductions in the emissions of

pollutants. A central authority (a governmental body) sets a limit or cap on the amount of a pollutant that may be emitted. The limit or cap is allocated or sold to firms in the form of emissions permits which represent the right to emit or discharge a specific volume of the specified pollutant. Firms are required to hold a number of permits equivalent to their emissions. The total number of permits cannot exceed the cap, limiting total emissions to that level. Examples of successful cap and trade programs include the nationwide Acid Rain Program and the regional NOx (oxides of nitrogen) Budget Trading Program in the Northeast. The principal pollutants associated with gas turbines are NOx. Consequently, these types of environmentally friendly taxes financially motivate gas turbines control strategies for NOx. Those strategies nowadays include water or steam injection and premixed burners as well as the post combustion control by installing a catalytic reduction unit. It consists of reacting the NO with injected ammonia in the presence of a catalyst [2]. Control strategies incorporated within the combustion process often result in reduced combustion efficiency and thus increased emissions of carbon monoxide and unburned hydrocarbons. Consequently, the remaining goal for the gas turbines designers is to increase the combustion efficiency while reducing the pollutants formed within the combustor.

Furthermore, with the current changes in the fuel sources, burners should now be adapted to alternative fuels besides decreasing pollutant generation. Indeed, recent modifications in our approach of the fuel sources bring new considerations. Stability in the combustion system is a decisive point on aircraft combustors in which a flame should be controlled over miscellaneous conditions during the flight. The localization and diversity of the alternative fuel source candidates in ground power generation also

requires the development of stable fuel-flexible combustion systems. Thus, the logical gas turbine market expectation for new products is to maintain reliability with a low environmental impact and a high level of fuel adaptability.

Nitric Oxides Reduction

As we explained, the emissions abatement is of primary significance for both power generation and aircraft propulsion systems. Nowadays, combustors use NOx-reducing techniques. This includes special forms of combustion such as new flameless configurations [3] which allows us to avoid temperature peaks within stabilized flames in order to mostly suppress NO-formation. Different mechanisms have been identified in the generation of Nitric oxides such as the Zeldovich [4] or thermal NOx mechanism. Overall, NOx emissions are strongly linked to the flame temperature. There are three predominantly sources of nitric oxides from combustion processes: prompt NO, fuel NO and thermal NO. The main source is the thermal NO-formation, described by the 'Zeldovich-mechanism'. The three principle reactions for this formation are:

$$O + N_2 \leftrightarrows \mathrm{NO} + \mathrm{N}$$

$$N + O_2 \leftrightarrows \mathrm{NO} + \mathrm{O}$$

$$N + OH \leftrightarrows \mathrm{NO} + \mathrm{H}$$

As indicated in its name, the higher the temperature is the more significant the thermal NO-formation is. Significant NO emissions can be found if oxygen containing combustion products are exposed to temperatures:

$$Temperature\ (°\mathrm{C}) > \begin{cases} 1600, & for\ seconds \\ 2000, & for\ milliseconds \end{cases}$$

Because of that strong temperature impact, most NO-reducing techniques try to remove peak temperatures by keeping the residence time in high temperature areas low and by avoiding high oxygen concentration in these zones. Flameless oxidation has been variously termed: dilute combustion, moderate and intense low oxygen dilution (MILD), lean combustion, homogeneous combustion and low NOx injection.

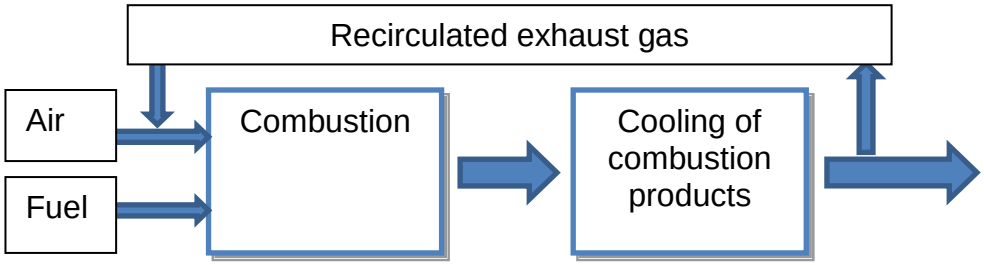

Figure 1-1. NOx-reducing by exhaust gas recirculation

Contrary to the combustion in stabilized flames, the combustion at flameless oxidation is temperature and mixture controlled, reached by precise flow and temperature conditions. A stable flame requires a balance between flow and flame-velocity. This is true for premixed as well as diffusion flames.

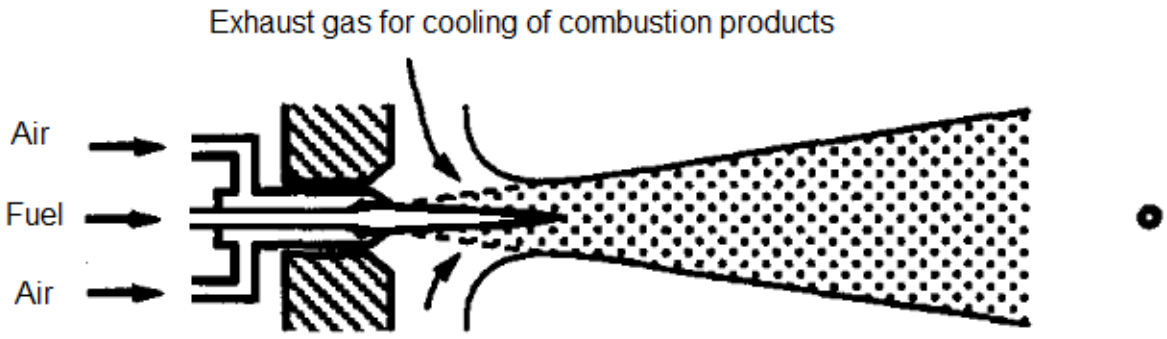

Figure 1-2. Schematic stable flame

Stable flames are conceivable over the whole range of combustion chamber temperature but only for recirculation rates up to 30%. For higher recirculation rates,

below the mixture self-ignition temperature, the flame will become unstable, lift off and finally blow out.

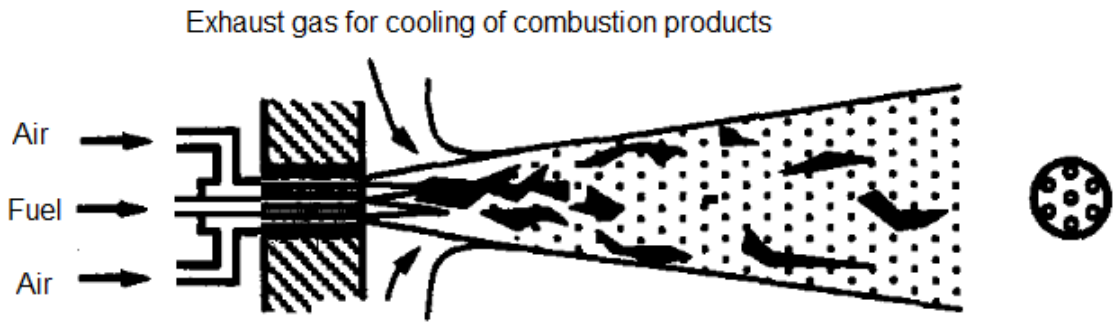

Figure 1-3. Schematic unstable flame

Combustion instability also referred to as unsteady flow oscillations, is a common problem, and slowed down the development of lean-premixed combustors. These oscillations may reach sufficient amplitudes to interfere with engine operation, and in extreme cases, lead to failure of the system due to excessive structural vibration and heat transfer to the chamber. The narrow range of stability offered by premixing compared to diffused burners makes lean premixed technology difficult to implement.

However, if the furnace temperature and the exhaust gas recirculation is sufficiently high, the fuel can react in the very steady, stable form of flameless oxidation. Emission reductions could be realized through the dry low swirl-stabilized combustion [7]. Moreover, the fuel to air ratio in the flame locally impacts the mechanism of soot formation. Thus, large gradients in the composition of the mixture increase the formation of soot precursors. Mixing the air and the pre-vaporized liquid fuel upstream of the injector creates a more homogenous mixture decreasing significantly the amount of soot precursors formed.

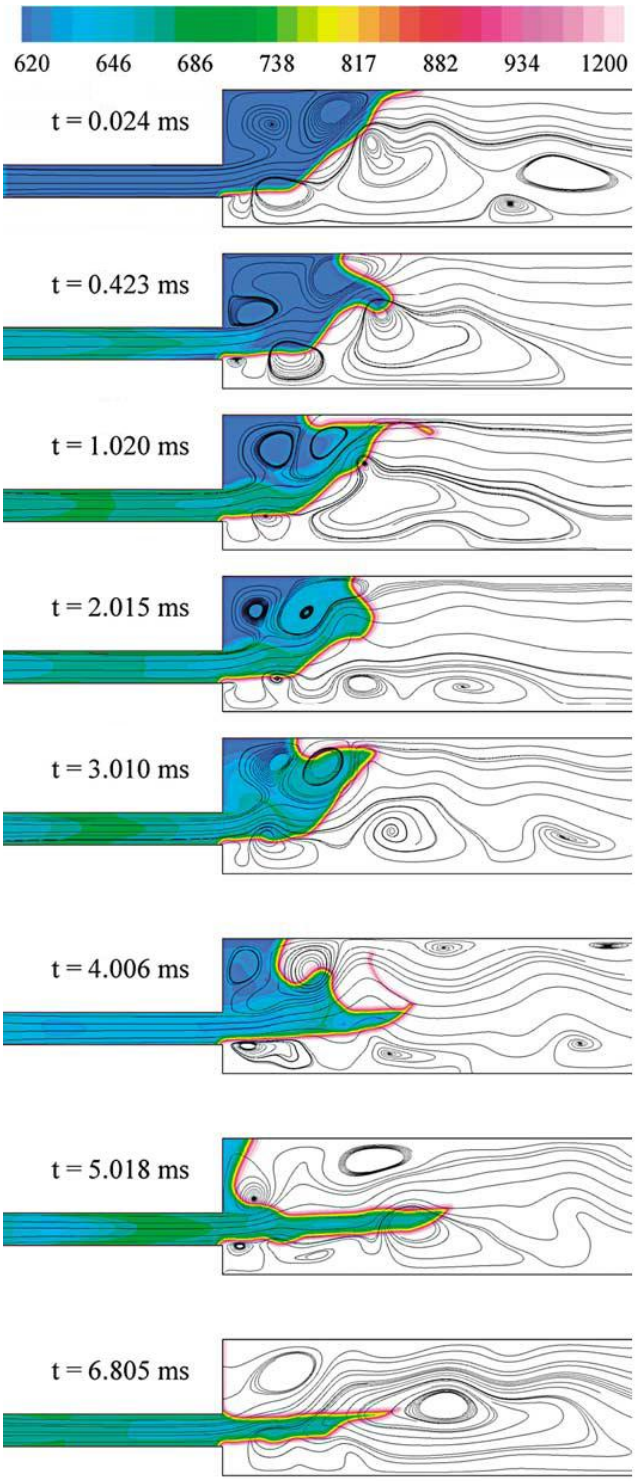

Figure 1-4. Transition from stable to unstable flame due to changes in flow conditions [5]

Figure 1-5. Burner assembly damaged by combustion instability and new burner assembly [6]

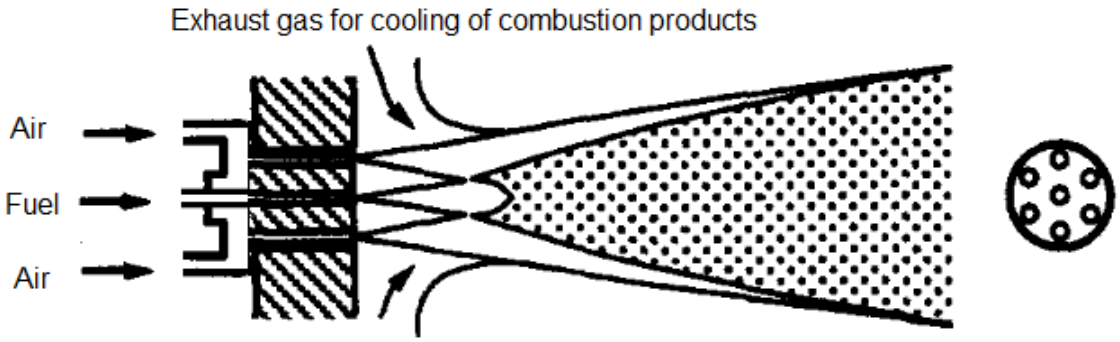

Figure 1-6. Schematic flameless oxidation

On the figure 1-6, a schematic representation of flameless oxidation, the gas is supplied axially through the central gas nozzle and the air is injected through concentric arranged nozzles. Because of the distance of gas and air supply, the reaction could only take place further downstream, when a large amount of exhaust has already mixed in. An additional objective in aircraft propulsion engines development, very conventional, is to scale down the combustion systems. Basically, we are looking for the highest heat release in the smallest volume. By reducing the weight, we also reduce the overall fuel

consumption. But then we create an extra difficulty for the cooling system. Indeed we have to avoid local temperature peaks in a small volume with high heat release. With our experimental combustor we need to be able to identify a flameless combustion configuration. Relevant characterization measurements for this type of combustion are temperature and NOx concentration. Arbitrary, while burning methane in our burner, we will be considering flameless configuration when both measured temperature is less than 1200°C at the exit of the annular space and measured density of NOx particles at the exit of the burner is below 5 ppm.

Synthetic Gas and Fuel-Flexibility

As we mentioned it, the contemporary energy context offers a stimulating force for exploration of alternative sources of fuels such as biomass and coal, as fossil fuel supplies decline. An environmentally friendly alternative gaseous fuel for internal combustion engine mainly consisting of carbon monoxide (CO) and hydrogen (H2) called syngas is nowadays able to substitute fossil diesel oil in combustion engines. Nevertheless, coal-derived synthesis gas like syngas present combustion characteristics relatively different from deeply examined methane. In addition fuel sources will possibly become progressively local as the diversification of sources becomes a truth, and thus the composition of the syngas is likely to be highly changeable. Hereafter, there are durable motivations to develop technologies to enable the safe and efficient use of alternative fuels in aircrafts as in other transportation and power generation engines. The premixing concept used in dry low NOx systems is particularly sensitive to the composition of the fuel used. We already briefly described how changes in fuel composition impact the emissions and heat release performance

inside the burner, but it also has an influence on the other components of the fluid path such as the compressor and the turbine. Indeed, increase in air flow rate due to a lower heating value of the burning mixture may affect the compressor performance. This is easily observable such as in the computational analysis of centrifugal compressor surge control using air injection realized by A. Stein, S. Niazi, and L. N. Sankar [8]. They used as a specific configuration to investigate instabilities a high-speed centrifugal compressor. They developed and used a Navier–Stokes solver for simulating unsteady viscous fluid flow in turbo machinery components to study fluid dynamic phenomena that lead to instabilities in centrifugal compressors. These studies indicate especially that large flow incidence angles, at reduced flow rates, can cause boundary-layer separation near the blade leading edge.

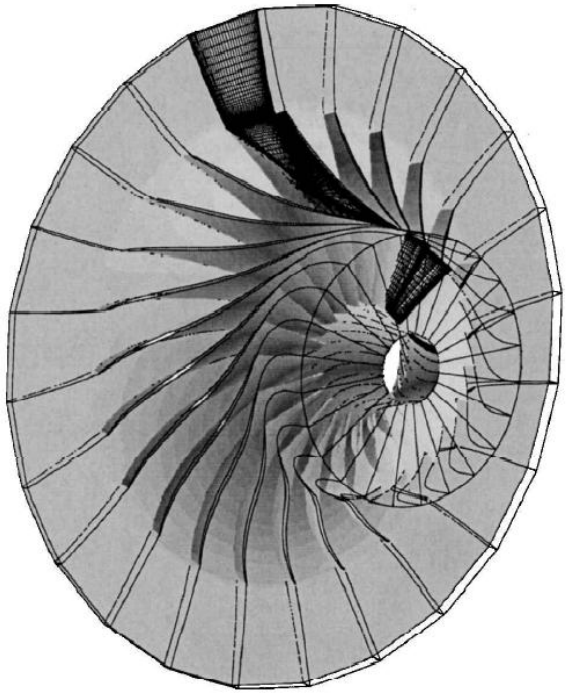

Figure 1-7. Single flow passage computational grid for a high-speed centrifugal compressor (dim 141x49x33 in the streamwise, spanwise and pitchwise directions) [8]

Additionally, the computational analysis of this centrifugal compressor gives us an idea of the influence of a change in flow rate over the compressor performance both through a simulation and experiments. This is illustrated in figure 1-8 and should definitely be considered to fully take advantage of the novel fuel flexible technology burner hypothetically implemented into a gas turbine engine.

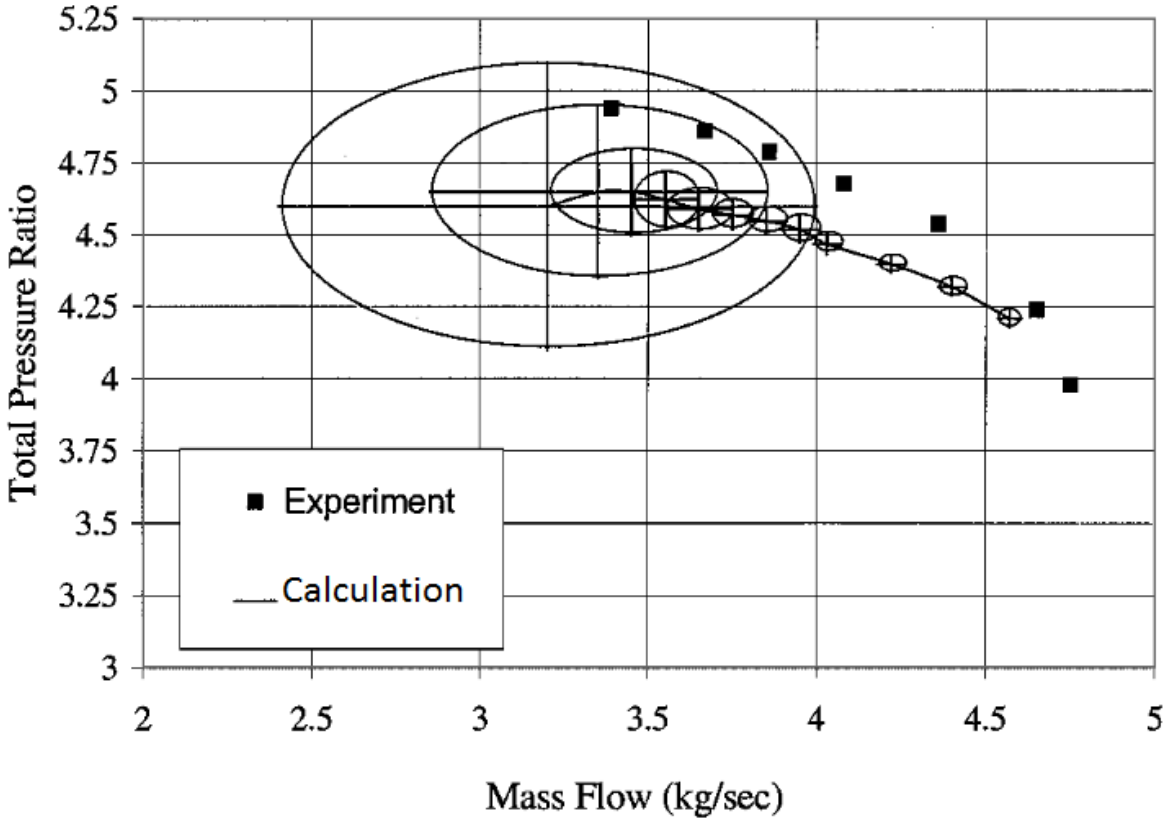

Figure 1-8. Calculated and experimental performance map of a a high-speed centrifugal compressor

In the same way, corrosive products might also be an issue in material wear when designing a gas turbine with a fuel flexible burner. In premixed systems, the oxidation chemistry plays a significant role. As a result, operability and emissions performances are greatly influenced by the gas composition. In these premixed systems, the mixture of air and fuel is flammable far upstream of the injection point. As a consequence, the

ignition delay has to be sufficiently controlled not to let the ignition arise in an unpredicted area of the combustor. Unexpected ignition could produce potentially critical effects. An even more important critical accident that we have to avoid while implementing our burner is a flashback on the air supply lines. Investigations have been made on the chemistry dynamics in order not to accidently reach any combustion limits (excess of lean or rich combustion) while slightly changing operating conditions. An experimental approach of these investigations is described in the fourth chapter “experimental calibration”. Measurements have been done to study the oxidation of various exotic gas through diverse experimental set ups and compared with computer simulations exposed in B. Fond’s thesis [1]. Datas on the oxidation and pollutant formation kinetics could be extracted from diverse measurements such as flame blowout, ignition delay and laminar flame speed. Shock tube experimentations have been studied broadly and ignition delay relationships have been extracted for several fuels over a wide range of conditions. The ignition delay is relevant to consider in the implementation of the fuel flexible combustor since this delay is significantly impacted by changes in the gas mixture composition. Basically, an auto-ignition phenomenon [9] at an undesired place could clearly damage the combustor. Z. ZhenLong and coworkers have developed correlations for the ignition delay times of H2/air mixture [10]. The hydrogen/air ignition delay times for initial conditions over a wide range of temperatures from 800 to 1600 K, pressures from 0.1 to 100 atm, and equivalence ratios from 0.2 to 10 were estimated and modeled using the method of high dimensional model representations. These specific auto-ignition delays have been very-well investigated. D. M. Kalitan, J.D Mertens, M.W. Crofton and E. L. Petersen have studied ignition

delays of CO/H2/air mixtures behind reflected shockwaves at atmospheric conditions and elevated pressures [11]. They paralleled their experimental measurements to existing kinetic models. This kind of considerations appears to be an essential precursor to the use of synthesis gas in power generation plants on a wide scale. Undeniably, H2 and CO have especially low flammability limits and the combustion rates of a synthesis gas mixture are strongly associated with the H2/CO ratio. Shock tubes experiments results are obviously coming from transient process experiments, but ignition delays can similarly be obtained from constant flow devices and rapid compression measurements machines.

The laminar flame speed model for premixed laminar flame combustion contains information on the kinetics of the combustion of the mixture. It also contains information on the diffusivity of its species, and related thermo chemistry [12]. Natarajan and coworkers burned CH4/H2/CO mixtures in Bunsen burner and wall stagnation flame reactors. They achieved flame speed measurements with a charge coupled device camera on the Bunsen flame, and laser Doppler velocimetry on the stagnation reactor. Premixed mixtures went from 5-95% for H2 and CO and up to 40% for CH4, and measurements have been done on preheated mixtures up to 700K, and at pressures ranging from 1 to 5 bars. Measurements could then be compared with some detailed methane oxidation mechanism such as the Gas Research Institute mechanism version 3 (GRI Mech 3.0). Detailed mechanism provides with kinetic rates of elementary reactions such as thermo chemistry of the species involved. The GRI 3.0 describes a detailed mechanism appropriate to gas natural combustion. It includes the NOx formation and reduction but does not describe soot formation [13]. In addition, lean

blowout measurements are often done on premixed pre-vaporized swirling flame combustor devices. Based on the concept of chemical time limited reaction, the residence time of the reaction at blowout could be linked to the reaction rates and compared with a reactor network model. Zhang et al. studied the effect of the composition of H_2/CO/CH_2 mixtures on lean blowout in a premixed gas turbine combustor. Nevertheless, a nonhomogeneous reaction zone will produce other combustion regimes than the lean blowout theory such as flamelets into eddy.

Well Stirred Reactor

Longwell and Weiss designed the first device approaching the well-stirred reactor concept in 1953 [14]. In order to separate the convective and diffusive physical processes from the chemical reactions; an appropriate mixing must be reached such as in a well stirred reactor. Overall, the well-stirred reactor concept is largely used as a modeling tool to study reactor behavior.

In this type of reactor, the composition is assumed homogeneous. Consequently, the exhaust mixture composition is the same as the composition in the burner. The assumption of homogeneity is relevant in the case of our reactor since mixing forces generated by the velocity jets are significant. The idea is that a residence time of the gases inside the reactor could be extracted which would put together the influence of the incoming flow, the temperature, the pressure inside the reactor and the volume of the reactor. This residence time could be given by the expression below:

$$t_{res} = \frac{\rho V}{\dot{m}} = \frac{PV}{\dot{m}RT}$$

This time represents the delay acceptable for the chemical reaction to progress toward completeness; in this case the maximum reaction rate is preceding blowout. Experimental blowout measurements were performed within our burner for rich and lean mixtures and compared to theoretical ones.

The numerical well-stirred reactor model of our burner previously established and described in chapter 5 is considering the burner within a steady state with a steady incoming flow and uniform properties over its volume. The modeling equations used are derivate from the Reynolds Transport Theorem, respectively the continuity equation, the energy equation and the rate laws. They could be expressed as below:

$$\dot{\omega}_i MW_i V + \dot{m}(Y_{i,in} - Y_i) = 0$$

$$\dot{Q} = \dot{m}_i \left(\sum_{i=1}^{N} Y_i h_i(T) - \sum_{i=1}^{N} Y_{i,in} h_i(T_{in}) \right)$$

$$\dot{\omega}_i = \sum_k f_k(T, P, Y_j)$$

In chapter 4 we will observe the direct influence of the residence time over the NOx particles emission when our combustor is running under stoichiometric conditions.

CHAPTER 2
STATEMENT OF SCOPE

Burner Specific Geometry

The geometry of this burner, previously described in the B. Fond's thesis [1], allows a sufficient amount of back mixing in order to stabilize the flow and to provide a good homogeneity. It has been designed in order to let the air and fuel flows fully mix before combustion. This is part of the reduction in CO and NOx emissions in new gas turbine combustors strategy introduced before. Along with low CO and NOx emissions, the significant low gradients in fuel/air fraction of the mixture entering the primary zone also prevent the formation of hot spots responsible for the formation of polycyclic aromatic hydrocarbons (PAH). Studies on premixed laminar flames showed that soot occurred only beyond a highly rich equivalence ratio [14][15]. The figure 2-1 illustrates this point, and gives us an illustration of the kind of impact on soot formation a rich equivalence ration could have on the chemistry of combustion.

Developments in modeling soot formation and burnout in combustion systems are surveyed [16]. The types of models are divided up into three classes: empirical, semi-empirical and detailed. Empirical models use correlations of experimental data to predict trends in soot loadings. One of these models, the ionic theory for soot formation is a theory primarily advocated by Calcote [17]. Calcote and coworkers have supported the prominence of a link between ions in flames and soot formation. Excellent arguments and data have been presented showing a strong connection between soot and ions. This is schematically illustrated in Figure 2-2. The theory suggests that formation of soot origins from a sequential growth of ions starting with the ions $C_3H_3^+$.

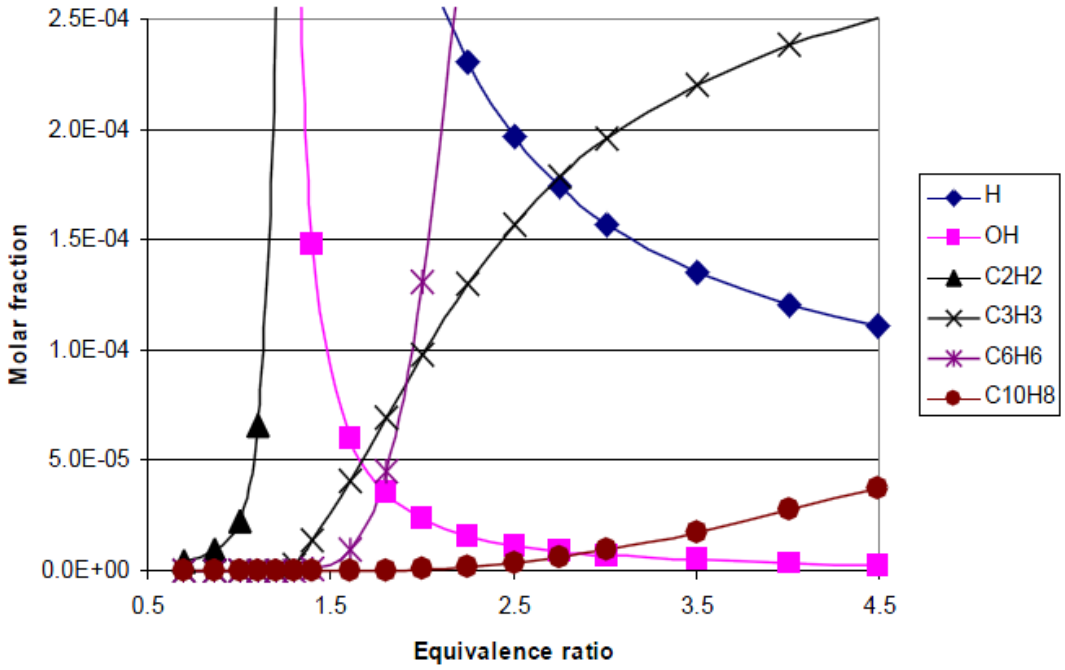

Figure 2-1. Dependence of H, OH,C3H3,C2H2, benzene and naphthalene concentrations on equivalence ratio for ethylene combustion (1650K, 1 atm)

The first three reactions of Calcote's mechanism for soot formation have fully been studied.

$$C_3H_3^+ + C_2H_2 \leftrightarrows C_5H_5^+$$

$$C_5H_5^+ \rightarrow C_5H_3^+ + H_2$$

$$C_5H_3^+ + C_2H_2 \leftrightarrows C_7H_5^+$$

The first of the three reactions is reversible and involves the formation of a specific encounter complex sensitive to pressure and ion kinetic energy. The second reaction appears to require large amounts of internal energy in the $C_5H_5^+$ ion in order to

proceed. The third reaction is reversible; nevertheless, in contrast to the initiating reaction, the $C_5H_3^+$ ion formed from the $[C_7H_5^+]$* complex exhibits a much lower reactivity.

However, premixing also brought stability issues in homogeneous mixtures, particularly as they operate near lean blowout. Stabilization techniques, such as bluff body and swirlers have been seen as a way to achieve significantly stable operation at low equivalence ratio. Re-circulating combustion gases transfer heat to the cool mixture, raising it to the auto ignition temperature. The stabilization performance depends on the time for the cold mixture to enter the shear layer limiting the recirculation zone, the rate of entrainment of fresh mixture into the recirculation zone, and the residence time of gases inside the recirculation zone.

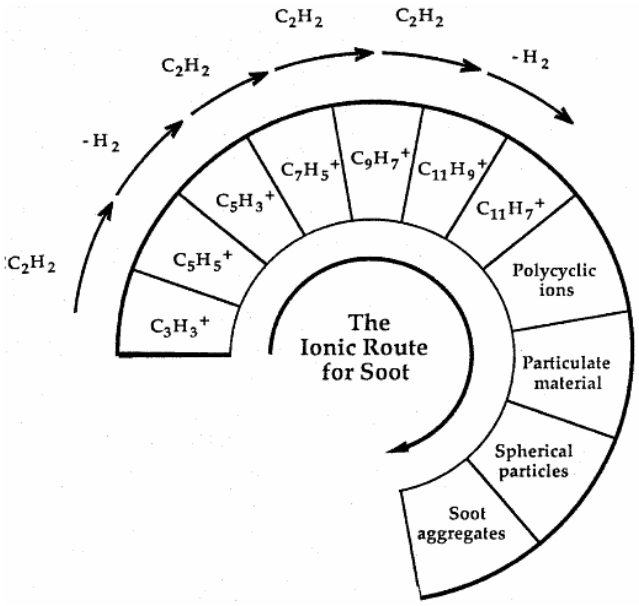

Figure 2-2. A schematic illustration of soot formation according to the ionic theory [17]

However, in swirl-stabilized flames, vortex precession and breakdown phenomenon would be an important source of combustion instabilities so hat active boundary control and Helmholtz resonators are often employed in current dry low NOx technologies [1]. The idea behind the current design is to provide back mixing based on jet impingement and flow split rather than large vortices structures.

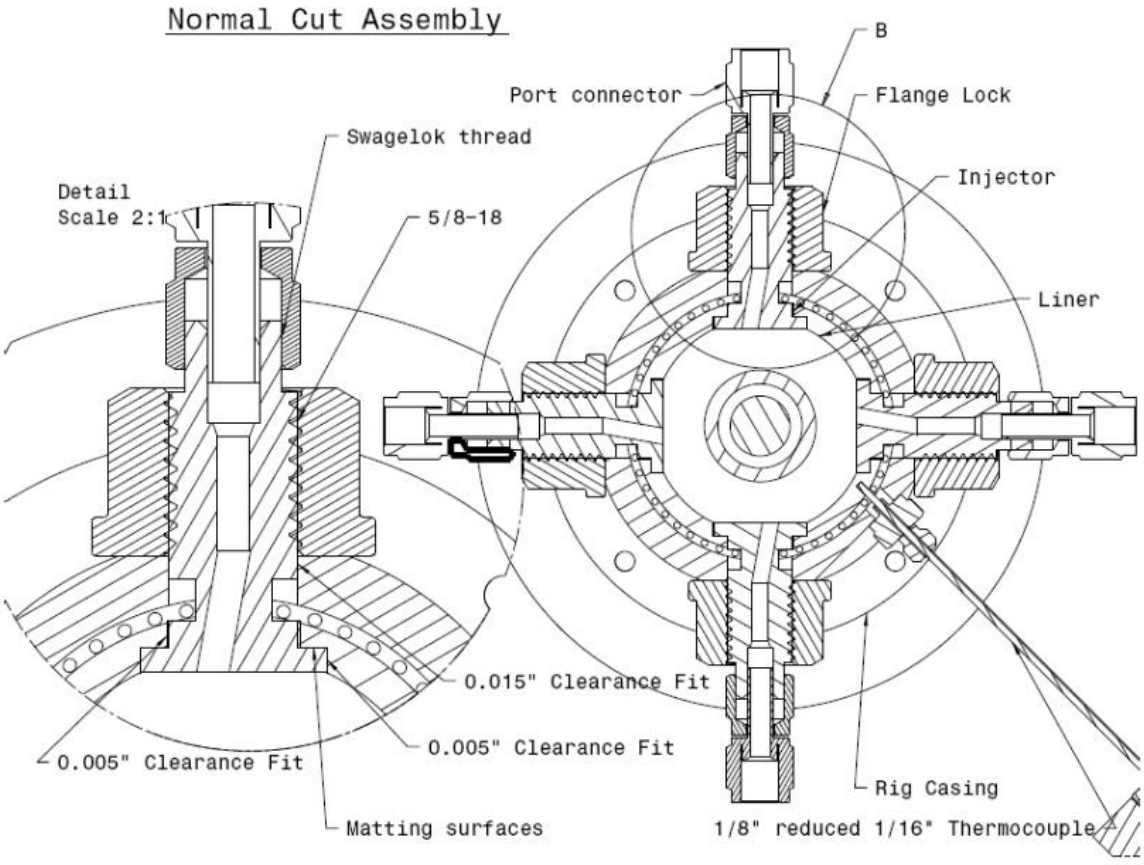

Figure 2-3. Normal cut of B. Fond's burner

The combustion zone geometry of B. Fond's burner has been elaborated to provide this low velocity recirculation zone. This geometry is shown on Figure 2-3 and Figure 2-4.

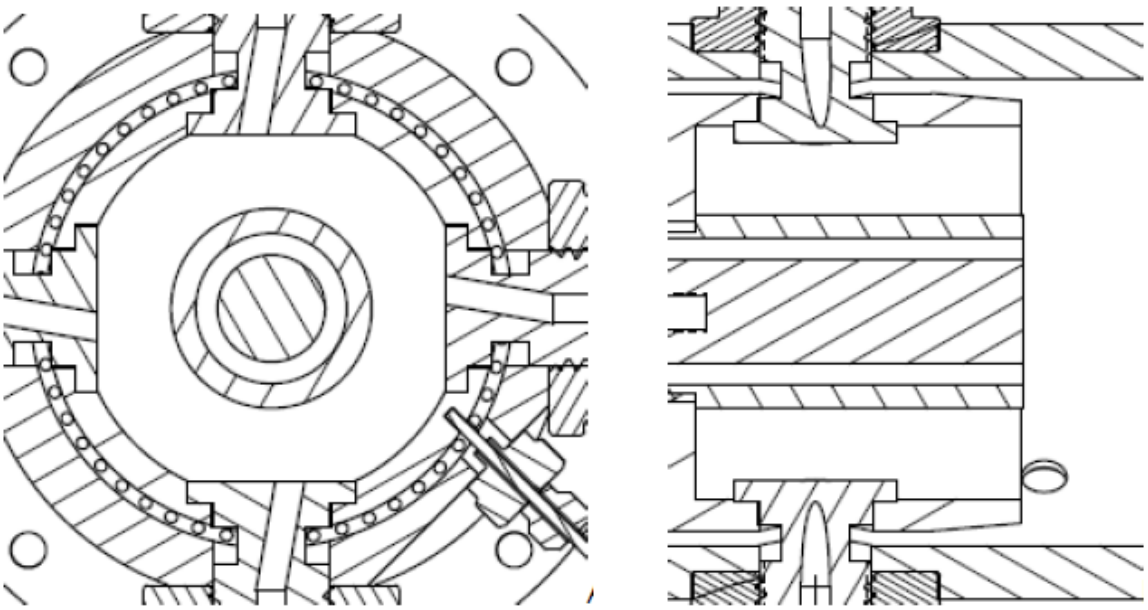

Figure 2-4. Cuts of B. Fond's combustion chamber

The annular combustor presented here is made of a hollow cylinder liner with a wall on one side and the exhaust on the other side. A smaller tube is mounted and the mixture is injected almost radially somewhere along the length of the liner. The fresh mixture will come in at a relatively important speed into the central tube so that part of it will be entrained near the rear wall and the other part will go in the direction of the exhaust where it will be later diluted with the liner cooling air. This design will provide a cross flow between the injection stream and the combustion products coming from the back of the reactor and so the heat transfer and mixing will be enhanced.

In this design two parameters were incorporated to address geometry influences. The inner tube can be replaced, changing considerably the jet impingement configuration as well as the combustor volume. In addition, the injectors are cylindrical and incorporate a slight 10° injection angle with respect to the radial direction so they

can be rotated to act on the flow split as show in figure 2-4. The swirl number is defined in the equation:

$$S = \frac{\int_{r_i}^{r_0} \rho U_\theta U_z r^2 dr}{\int_{r_i}^{r_0} \rho {U_z}^2 r^2 dr}$$

Where U_θ and U_z are respectively the tangential and axial velocities, r_i and r_o the inner and outer radius of the annular space. Considering the cold gas injection velocity and the combustion product axial velocity, the swirl number could be approximated at 10. However, the high velocity of the cold mixture jet imply a stirred reaction zone more than a swirling flow.

In this design, air and fuel are injected at four different points around the circumference and the jets are directed toward the center tube. The number of injectors has been seen as the simple way to provide a good homogeneity and a good control over the reactor composition by opposition to a liner with holes. It revealed stability performance.

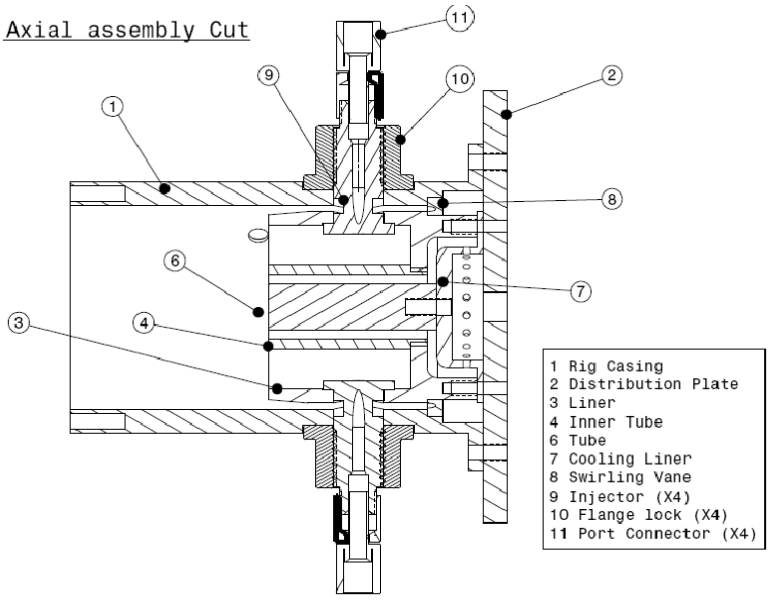

Figure 2-5. Axial Cut of the combustion chamber

Operating System Design

This novel combustion rig is located in the building 241 at the Research energy park of University of Florida. It includes all gases and fuel supply lines and an electric gas exhaust chimney. On its way to the mixing section, air is compressed, stocked, metered, and preheated. The liquid fuel will be pumped, metered, heated and sprayed into the combustion air stream. The mixture of syngas and combustion air is injected in the combustor primary zone. The flexible gas supply system allows us to simulate exhaust gas (CO2) injected with syngas. Some of the air goes directly to cooling passages (outer and inner flows) before to be mixed with the combustion products. Each single line is monitored in real time via Labview. After combustion, the streams are exhausted outside the building. The different systems designed and implemented around the combustion chamber are presented in chapter 3 “Implementation”. All these supply components were defined with respect to the combustor capacities. The four injection angles were originally chosen horizontal and clockwise as a compromise between a good tangential distribution of the flow and a jet impingement speed.

CHAPTER 3
IMPLEMENTATION

The In order to supply the combustion chamber, various materials have been implemented. The whole system could be described through subsystems such as:

- The outside air supply system including the compressor, dryer, fliters
- The inside air supply including vanes, monitored mass flow controllers, preheaters and premixing systems inside the building
- The gas supply system including its flexibility and adaptibility aspects, vanes, monitored mass flow controllers, and premixing components
- The liquid fuel subsystem including pumps and preheaters
- The computer interface
- The thermocouples measuring temperatures of the burner
- The gas analyzer measuring the composition of the exit gas

Figures 3-1 and 3-2 are pictures of the burner assembly. The appendix B represents a schematic map of the whole implementation. This chapter details the design of these subsystems. These were previously introduced in B. Fond research work [1].

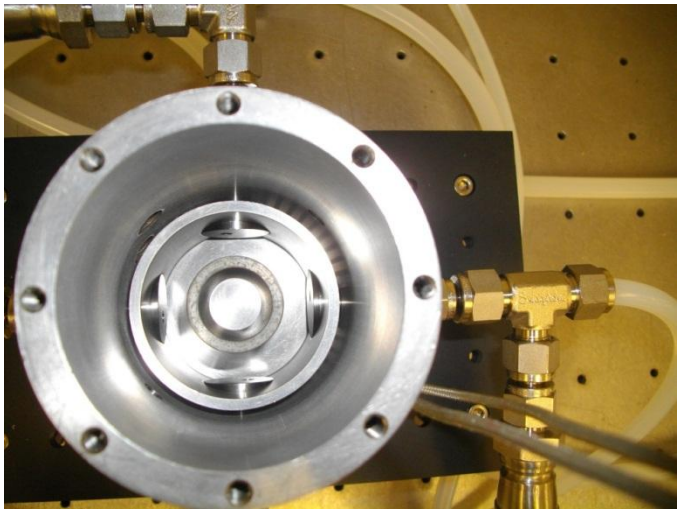

Figure 3-1. Picture of the annular combustion chamber from the top

Figure 3-2. Picture of the burner assembly

The Outside Air Supply Subsystem

The air supply has been designed to feed the combustion chamber with a constant flow whose composition, temperature and pressure are perfectly controlled. As we already mentioned it, at the premixed combustion section the fuel and air are mixed. The mixture arriving into the combustion zone is as homogeneous as possible. As also stated before, premixed combustion raised the problem of the presence of a flammable mixture downstream of the injector.

The list below of objectives had been established by B. Fond's dissertation [1]:

- Delivery of the combustion air flow to the four injectors (2-20g/s)
- Delivery of the cooling air to the cooling passages (inner and outer)
- Heating of the injection air to the desired temperature (400-700K)
- Atomization, Vaporization and mixing of the fuel in the air mixture
- Precise control over the four injector mixture composition.

The air supply line starts outside the building with the compressor pumping air to pressurize the outside tank with dried air. The maximum pressure the tank could support is 175psi. The compressor has been chosen according to the maximum gas flow needs in the laboratory site. We made the technologic choice to dry the air before letting it go into the tank. This allows us to stock already dried air but implied to lose the insurance of having freshly dried air. In order to make sure that stocked air stays dry we implemented a timer-activated electric moisture drain valves on the drain exit of the tank. The pressurized air supply is currently available for the whole building; it can now serve for other activities in the laboratory such as for example powering other combustion-based experiments. The idea at this point was to work on a duty cycle. Actually, the compressor is turned on immediately when the pressure in the tank drop under a specified charge. When the maximum pressure is reached the compressor is simply turned off. When we are operating the rig, the air flow is drawn from the tank on a continuous basis. Consequently, the pressure keeps decreasing in the tank until a specified minimum pressure is reached and then the compressor is turned on. The compressor could be modeled as a volumetric pump which means that the volumetric flow rate is constant and the pressure determined by the receiving tank pressure [1]. The tank could be represented as a constant volume system undergoing change in pressure.

A simulation of the pressure evolution in the tank is shown on Figure 3-3, which shows that the compressor could be turned on only 8 times when 35 SCFM are drawn to the combustor assuming a 200 gallons tank. An explicit Euler scheme could be used to represent the pressure evolution in a tank described below:

$$P(t+\delta_t) = P(t) + \frac{(\dot{m}_{in} - \dot{m}_{out})RT}{V_T}\delta_t$$

$$\text{Where } \dot{m}_{in} = \frac{P(t)}{RT}\dot{V}(t)$$

With V_T being the total volume of the injector and $\dot{V}(t)$ being equal to the volumetric flow rate of the pump when turned on or zero if turned off. The maximum pressure in the tank is set to 180 psi, which is the tank constructor rating and the minimal pressure at 80psi, so that the equipment downstream does not see too large of pressure variations. A dryer is used in line with the compressor to remove moisture and cool down to 50°F along with two high efficiency filters to remove small particles. The tables 3-1 is a list of the products that were ordered and implemented in order to realize this outside compressor part of the air supply line.

The figure 3-4 is a picture of the operational outside air supply system. We can see the Quincy compressor with its included little tank on the left, the dryer in the middle and the main tank on the right.

The Inside Air Supply Subsystem

The air supply subsystem inside the building has been implemented for an accurate control over the lines (gas and air) as well as for flexibility. This flexibility is

allowing staging and study of dissymmetry influences on stability. This also permits the simulation of injection of recirculated gas into the burner.

The four injectors composition are controlled separately for multiple reasons. The first reason is the capacity to run on a staged combustion regime on the long term, where two injectors run rich and two injectors run lean. The second reason is that one can study the effect of a perturbation of one injector on the global reaction regime, especially at low residence times. The last reason is the flow of air and fuel being fairly small; it would be difficult to have the composition fairly equal between the four injectors using some manual vanes.

Table 3-1. List of product for the compressed air supply outside the building

Product	Supplier	Description
QT 7.5-7.5.80	Quincy	Simplex air reciprocating compressor24.2 CFM at 175psi, mounted on an 80 gal. vertical tank
QPHT 50	Quincy	High inlet temperature refrigerated air dryer 40°F 40 SCFM with aftercooler and coalescing air filter.
CPNT 00030	Quincy	Standard coalescing filters at 30 SCFM and 100psig, 99% at 0.02 micron and with pressure difference gauge.
5018260-200	Quincy	120 gallons receiver tank
9831K13	McMaster	Clog-Resistant Timer-Activated Electric Moisture Drain Valves

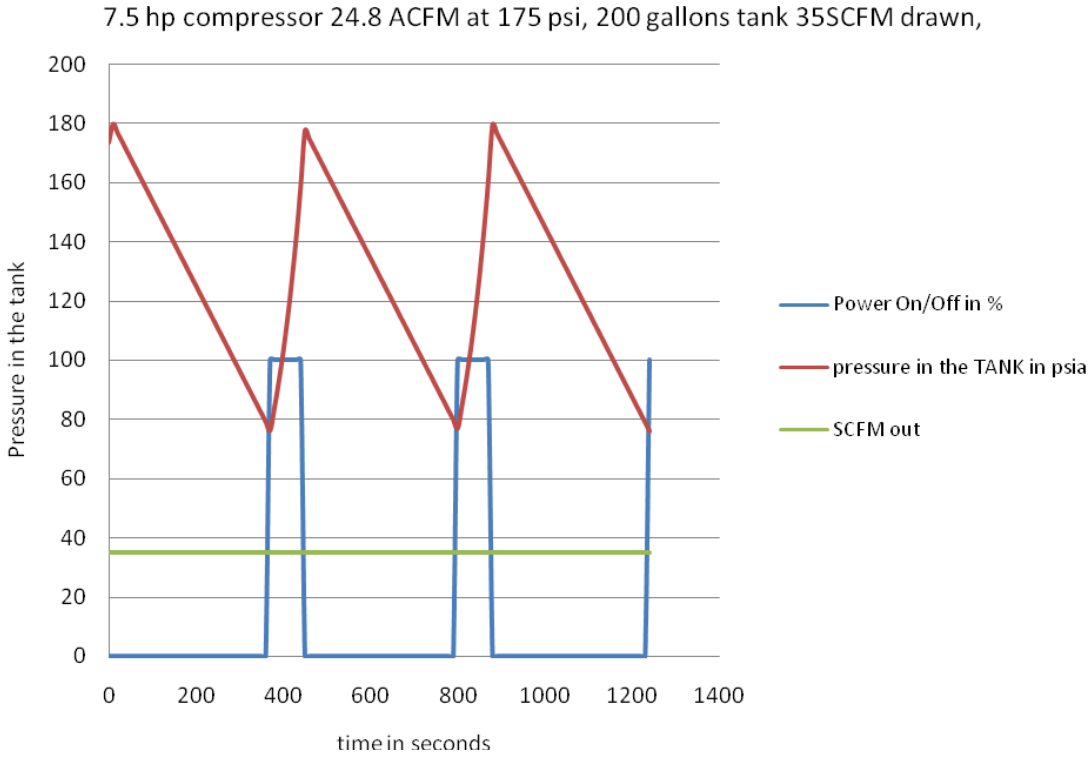

Figure 3-3. Pressure evolution in the tank at 35 SCFM

Figure 3-4. Picture of the outside air supply system

The implementation of diverse fuels is considered in this project. The fuels considered are methane, hydrogen and carbon monoxide. We also consider to be running in a diluted regime with mixtures of carbon dioxide, nitrogen and water vapor. The controllers have been chosen so that their total number is minimized, and give at the same time the maximum flexibility over the composition of the four injectors. The gas mass flow controllers selected are already calibrated for all the gases that we are using. These are controlled from a computer interface and allow various control strategies in order to permit accurate variations in the flow range. The table 3-2 is a list of the flow controllers implemented on this project.

The figures 3-5 and 3-6 are picture of the actual flow controllers once implemented. Another aspect of the inside air supply subsystem is that the air is preheated. Design specifications for the combustion system included preheating the combustion air to a temperature up to 700K for partial load (7g/s) and 400K for all loads.

Table 3-2. List of flow controllers for the Air and Gas supply

Fluid	Type	Flows	Flow rates	Controller Ref.	Quantity
Air	Cooling central	0-10g/s	500SLPM	MC500SLPM	1
Air	Cooling annular	0-20g/s	1000SLPM	MC1000SLPM	1
Air	Combustion reactant	2-30g/s	1500SLPM	MC500SLPM	4
Methane	Combustion reactant	0-1.5g/s	150SLPM	MC50SLPM	2
Methane	Combustion reactant	4 0-0.5g/s	50SLPM	MC250SLPM	2

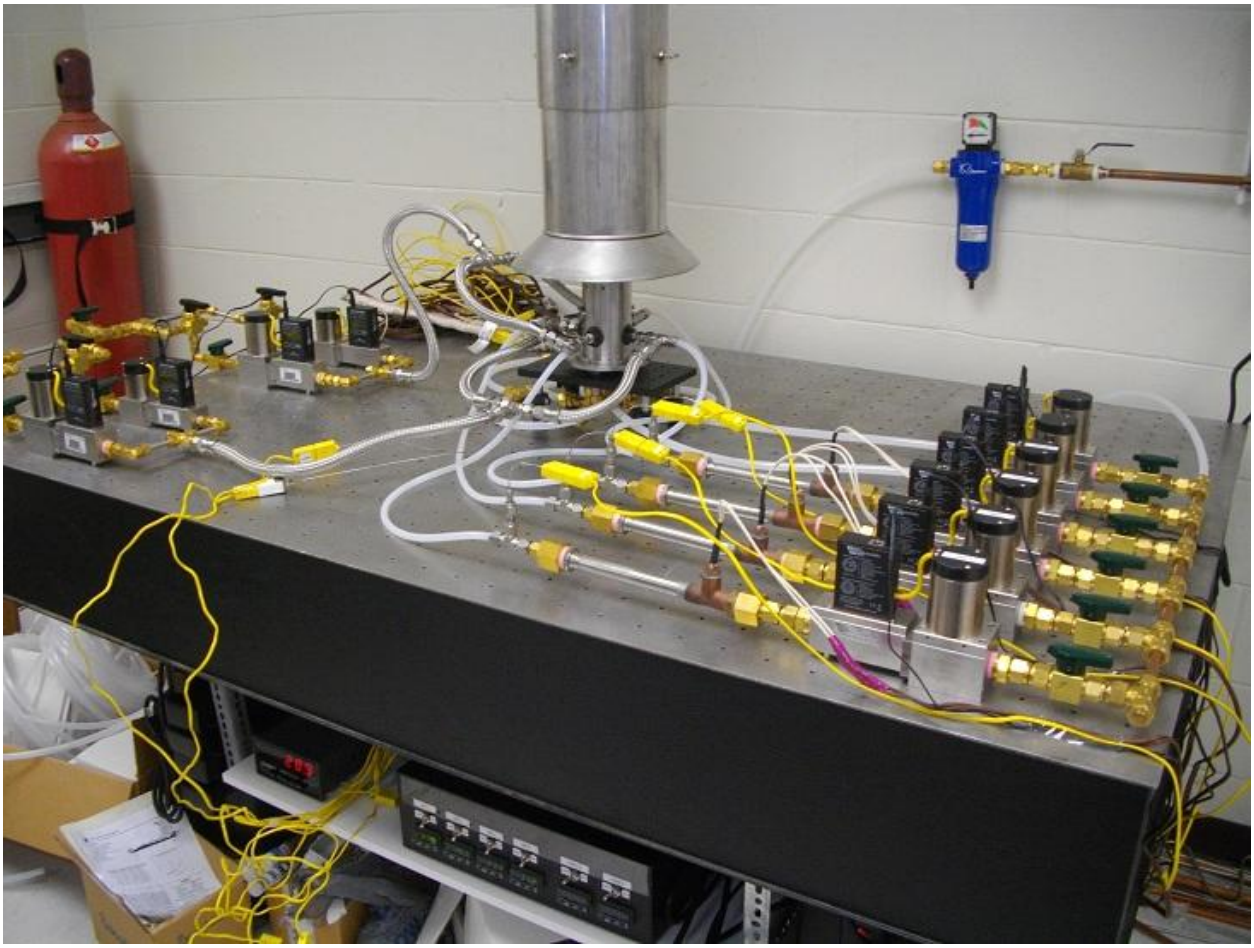

Figure 3-5. Picture of the flow controllers

Given cost considerations about flexible air lines able to handle such high temperatures, our choice was to use flexible silicone line and to limit as a first step the max preheating temperature of air to 630K. The available supply of air is about 750 SLPM which correspond to about 15g/s. With the four injectors being independently controlled, and the flow controllers not being able to withstand these temperatures, four independent heaters were used.

The energy equation could be used to estimate the power required:

$$\dot{m} C_p (T_{in} - T_{out}) = \dot{Q}$$

The air does not come directly from the dryer as mentioned before, it comes from the tank. Based on a 293K inlet temperature from the tank, the partial load at 630K requires 592 W and the full load at 400K, 403 W.

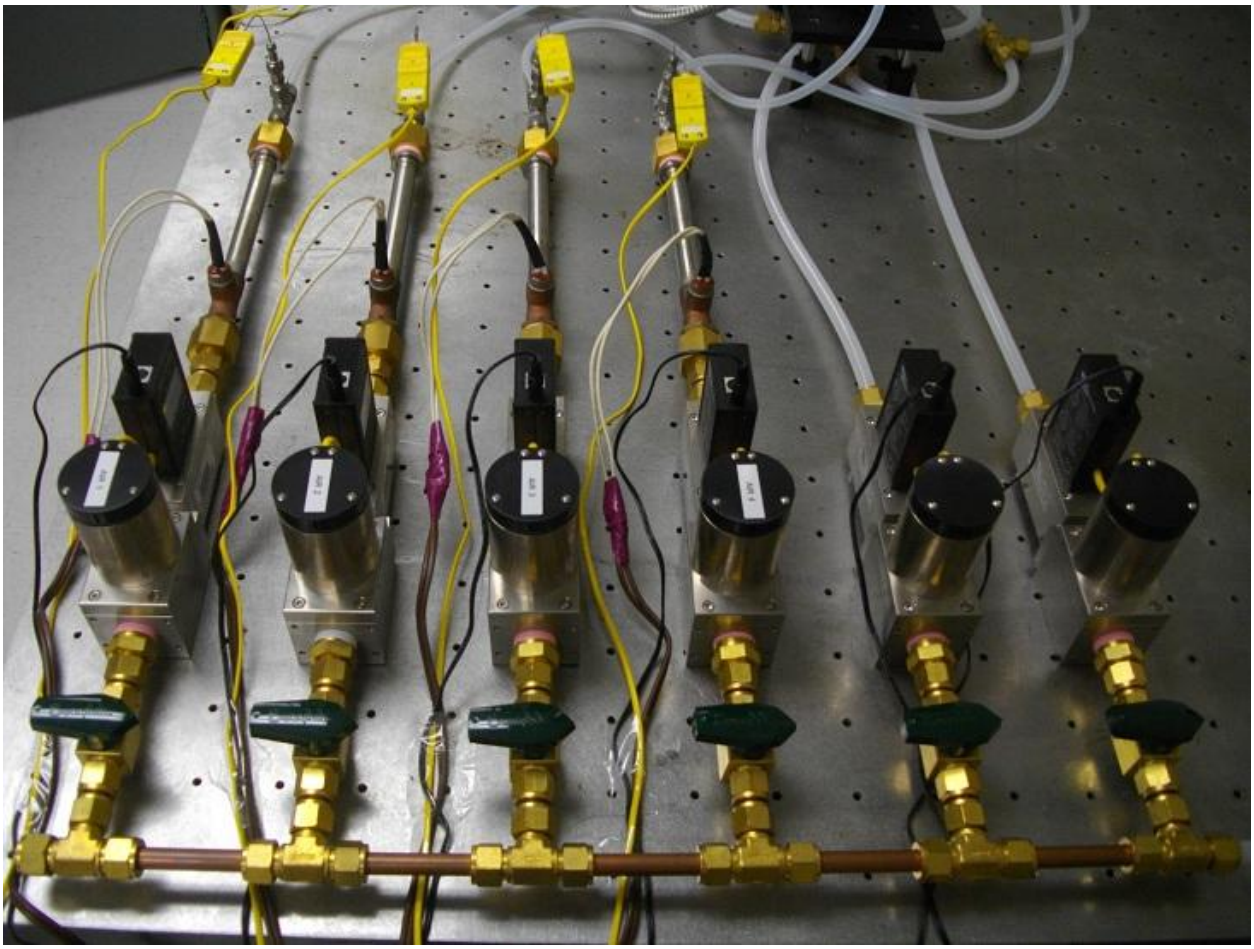

Figure 3-6. Picture of the flow controllers

The heaters are controlled on an ON/OFF basis using an auto tunable PID CN132 from Omega. These consider the difference between the set point and the signal of a type K thermocouple at the exit of the heaters. This controller being auto-tunable, it sets automatically the 3 constants of the proportional integral derivation action. The table 3-3 is a list of components realizing the preheating function. Figures 3-5 and 3-7 are pictures where one can observe of these components implemented. It is imperative for safety purpose to look at the way we built the pre-heating pipes. The thermocouples are

located at the exit of these pipes. This means that if the amount of air flowing through the pre-heated air lines is not significant the measured temperature will not be relevant. Thus a dangerous overheating of the air supply lines could occur without any significant regulation from the PID controller. In order to avoid this situation, we decided to program a safety minimum injected air flow of 4 SLPM per line into the computer interface.

Table 3-3. List of product for the air pre-heating system

Quantity	Device	Supplier	Model	Description
4	Air Heater	Omega	AHP 7561	T-Type heaters (750W)
4	Thermocouple	Omega	KQSS-116G-6	Type K thermocouples
4	Heater controller	Omega	CN132	PID Controllers
4	Controller relay	Omega	SSRL240DC10	Solid state relays

Figure 3-7. Picture of the control box operational

The Gas Supply Subsystem

We installed flow controllers and triple-way vanes such as shown on Figure 3-8 in order to realize the gas supply subsystem. This configuration allows multiple “flexible upgrades” to the current system. Indeed this allows us not only to flow other gas than CH4 such as H2 into the burner, but also to premix these gases in order to inject recomposed synthetic gas for example. It also gives us the possibility to inject CO2 which could be combined with preheated air to simulate exhaust gas recirculation. Given the high flammability of the gas that we are using, we secured the combustor gas supply lines. A kill-switch has been installed next to the rig, it allows us to stop the gas lines by shutting of the mass flow controllers power supply. It comes in addition with easily accessible physical vanes on the side of the rig table and numerical vane on the Labview interface.

The Computer Interface

The software used to create the computer interface is Labview. The current interface includes elementary safety options. Thus, the stop button acts directly on the gas supply lines to shut down the fuel supply without preventing the air from flowing through the combustor. The air flow controllers command board also includes a lower limit of air flowing to avoid the air preheating system to burn the pipes. Indeed with no air flowing the thermocouple located at the exit of the heating pipes would send a wrong temperature information to the PID controllers and may cause the pipe’s resistors to simply melt as described before. The Figure 3-9 shows the labview interface.

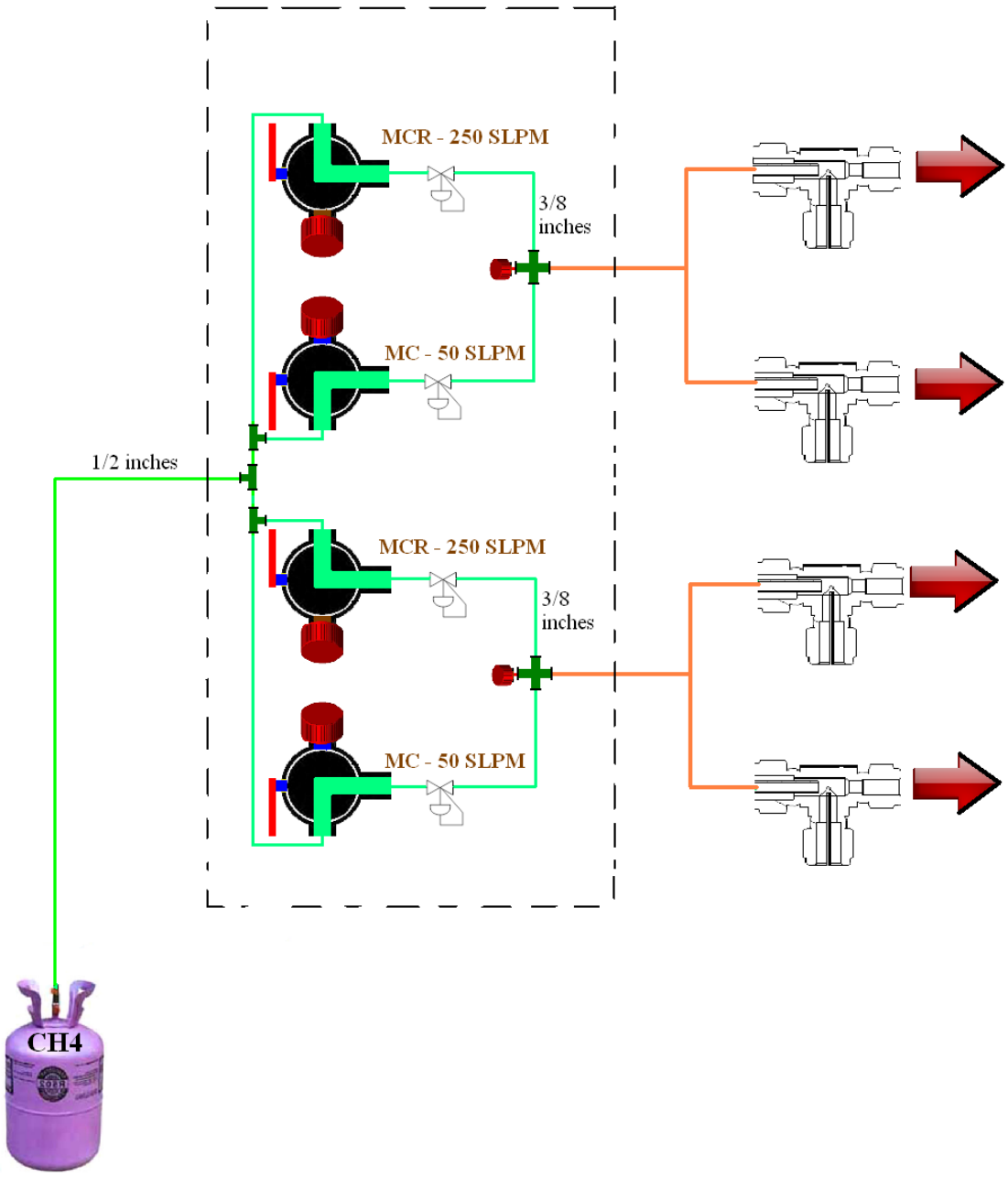

Figure 3-8. Gas supply flexible implementation

Figure 3-9. Labview interface

The Liquid Fuel Supply Subsystem

This subsystem has been realized using peristaltic pumps from Fisher Scientific and temperature control material listed in tables. We can observe the material of the subsystem on Figure 3-10. A description of the material used is given Table 3-4.

Table 3-4. List of material used for liquid fuel

Quantity	Device	Supplier	Model	Description
4	Flexible Heater for liquid fuel	Omega	STH051-020	Heavy insulated heater tapes 156W
4	Peristaltic pump	Fisher Scientific	13-876-2	Medium flow(0.8-85mL/min)
2	Thermocouple fuel	Omega	TMQSS-040G-6	Type T thermocouples
2	Heater controller	Omega	CN132	PID Controllers
2	Controller relay	Omega	SSRL240DC10	Solid state relays

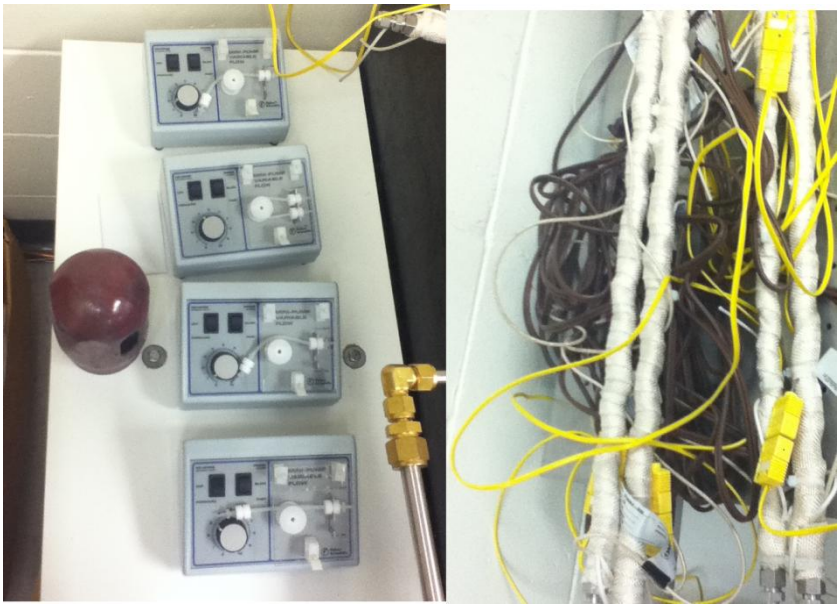

Figure 3-10. Liquid fuel supply subsystem

The Thermocouples

A mobile thermocouple able to reach the exit of the inner cooling flow, the outer cooling flow and the premixed air and gas flow was implemented. 3 thermocouples were implemented into the outer cooling flow. 2 thermocouples were implemented in contact with the external surface of the outer tube.

The inner cooling flow, the premixed gas/air flow, the outer flow, the inner tube, the outer tube and the rig case tube are shown on Figure 5-3.

The Gas Analyzer

A mobile gas analyzer has been used during experiments in order to measure the gas composition at the exit of out burner. For reasons previously described, we are particularly interested into measuring the NOx concentration. Limitations due to this device had to be taken into consideration, including the maximum temperature limit of 600 °C for the probe on a long run. The Figure 3-11 shows the gas analyzer used for experimentations.

Figure 3-11. Gas analyzer

CHAPTER 4
EXPERIMENTAL CHARACTERIZATION

Starting Procedure

The burner has to be started following a specific procedure. Indeed, its geometric design does not allow us to start it directly with a stable flame well-positioned into the annular space. When we turn on the burner, the flame has to be located at the exit, it implies that the initial ratio of gas injected over air injected has to be higher than stoichiometric. In addition, while running under rich conditions, no cooling flow (or extremely low inner cooling flow) is recommended. Once the flame stable at the exit of the burner, we have to wait few minutes to warm up the combustor. After this short delay, we have to slowly change the ratio of gas injected over air injected to come closer from the stoichiometric ratio. We are then able to observe the transition of the flame from the exit to the annular space.

Lean Blowout Limit

In order to observe clearly the lean operating limit of the burner for CH4, we fixed a total methane flow at 8 SLPM and the injected air flow at the stoichiometric corresponding flow. Then, we slowly increased the total injected air flow until the flame blowout. The results of the lean limit experimentation are detailed Figure 4-1 and Figure 4-2.

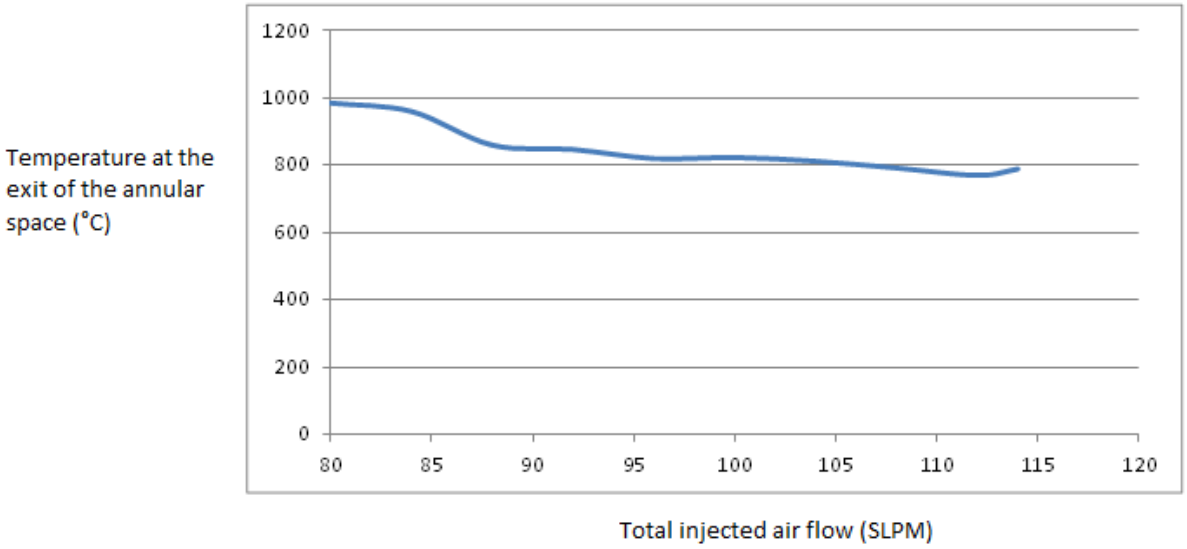

Figure 4-1. Graphic of the Lean Limit experimentation

			Thermocouple reference (°C)				
Total injected air flow (SLPM)	Inner cooling air (SLPM)	Outer cooling air (SLPM)	5	4	3	2	1
80	65	150	985	173	87	188	176
84	65	150	960	184	99	182	180
88	65	150	860	182	100	182	180
92	65	150	847	182	102	176	180
96	65	150	820	182	104	173	178
100	65	150	823	183	105	170	175
104	65	150	812	184	108	162	168
108	65	150	792	183	105	159	163
112	65	150	770	181	104	151	158
114	65	150	789	x	x	x	x

Figure 4-2. Table of the Lean Limit experimentation

Rich Blowout Limit

With the intention of observing the rich operating limit of the burner for CH4, we fixed a total methane flow at 8 SLPM and the injected air flow at the stoichiometric corresponding flow. Then, we slowly decreased the total injected air flow until the flame blowout. The results of the rich limit experimentation are detailed Figure 4-3 and Table 4-4.

On the Figure 4-3 we can observe that the temperature is going down when the operating ratio is close from the blowout one. On the Figure 4-1 it is hard to distinguish any relevant temperature profile. The reason is that during the experimentation the flame is moving with respect to the thermocouple. Indeed, while running lean the flame is transitioning from the annular space to the exit of the burner while the temperature probe does not move.

Nitric Oxides Emissions

With the purpose of observing the density of NOx at the exit of the burner running stoichiometric, we analyzed the composition of the exit gas. The results of these observations are available in Figure 4-5 and Figure 4-6. We can observe how NOx emissions decrease as the injected flows decrease. This is due to the fact that the mixture residency time into the annular space increases. We can also clearly notice that NOx emissions drop when cooling flows are increased

.

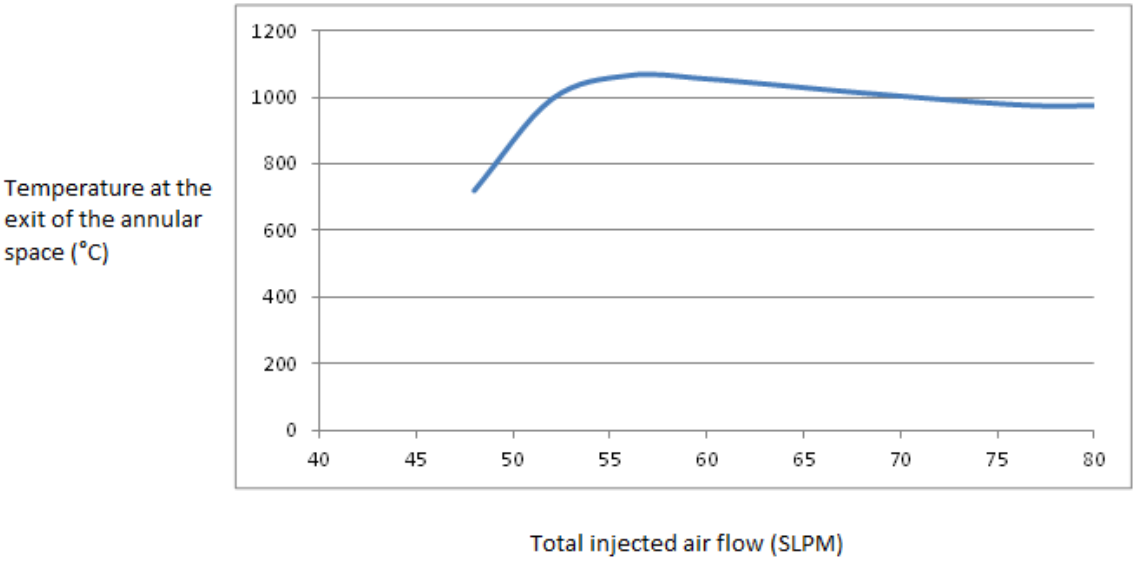

Figure 4-3. Graphic of the Lean Limit experimentation

			Thermocouple reference (°C)				
Total injected air flow	Inner cooling air	Outer cooling air	5	4	3	2	1
80	85	175	975	219	116	206	179
76	85	175	978	212	112	216	178
68	85	175	1014	204	108	241	175
60	85	175	1056	203	106	245	173
56	85	175	1066	183	97	198	146
52	85	175	995	151	82	101	106
48	85	175	720	114	68	75	73

			Thermocouple reference (°C)				
Total injected air flow	Inner cooling air	Outer cooling air	5	4	3	2	1
80	35	70	1009	244	132	264	249
56	45	100	1110	240	130.3	260	220
52	45	100	1015	185	107	132	145
51	45	100	1000	170	100	125	140
50	45	100	1010	170	98	130	148

Figure 4-4. Table of the Rich Limit experimentation

				Thermocouple(°C)								
Total CH4 flow	Total injected air flow	Inner cooling air	Outer cooling air	5	4	3	2	1	Nox(ppm)	Nox(mg/Nm3)	Nox(mg)	Power (kWatt)
4	40	10	30	900	155	94	104	140	6	3	0.252	2.66
6	60	15	40	970	230	140	246	253	18	9	1.089	3.99
8	76	25	50	1007	292	175	320	297	21	10	1.59	5.32
8	76	50	100	1000	275	152	303	263	2	1	0.234	5.32
10	96	50	100	1039	276	152	305	264	6	6	1.536	6.65
12	116	50	100	1070	295	161	328	287	16	8	2.224	7.99
12	116	75	145	1058	281	151	318	271	2	1	0.348	7.99
14	136	75	145	1085	283	151	319	269	6	3	1.11	9.32
14	136	100	200	1075	259	136	293	241	4	2	0.9	9.32
16	152	100	200	1105	266	135	300	243	4	2	0.936	10.65
16	152	145	300	1105	244	116	262	199	6	3	1.839	10.65
18	172	145	300	1122	239	111	264	201	6	3	1.905	11.98
18	172	175	400	1125	225	97	233	171	4	2	1.53	11.98

Figure 4-5. NOx Measurements

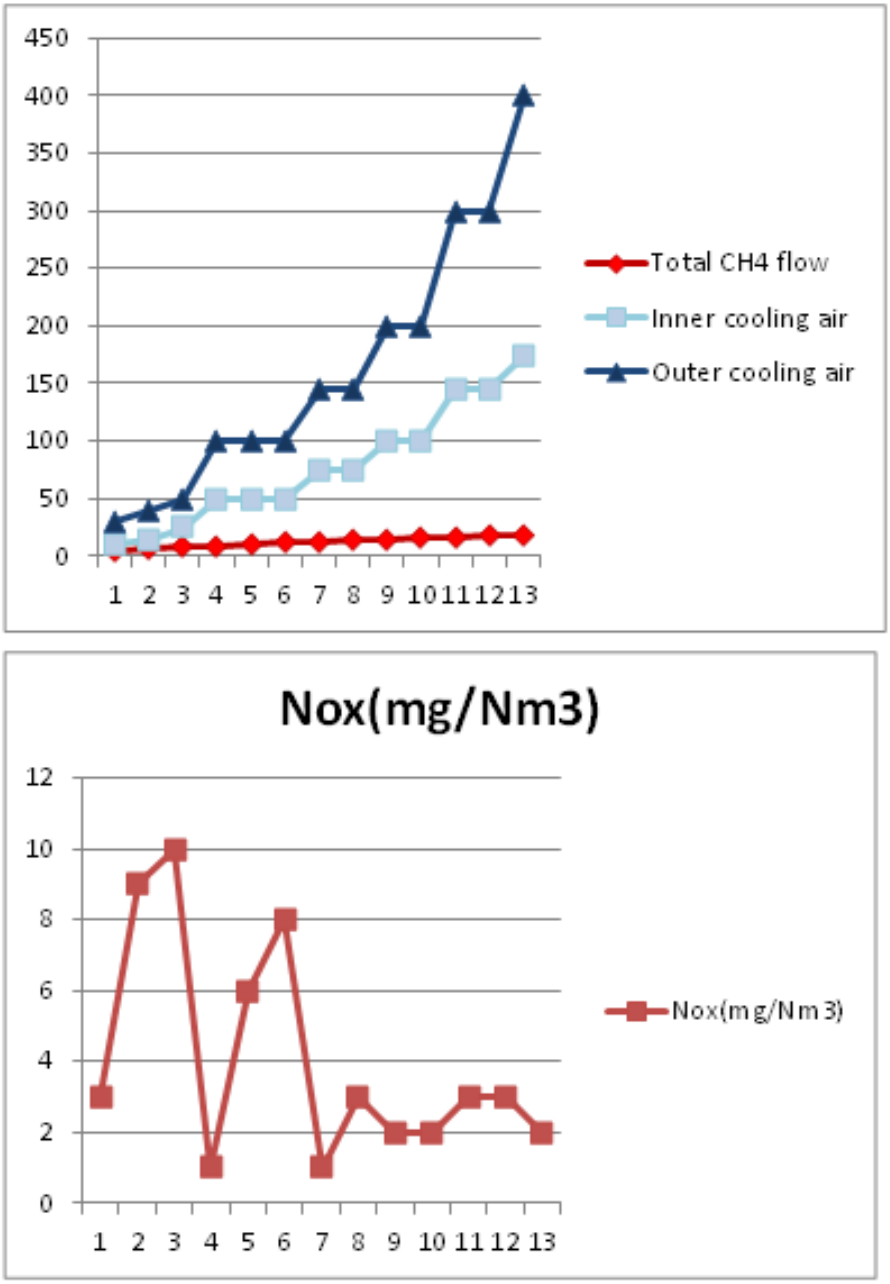

Figure 4-6. NOx Measurements Graphics

CHAPTER 5
DIFFERENCES BETWEEN MODELS AND EXPERIMENTAL RESULTS

Reaction Rate

The collision theory and empirical results provide the reaction rate expression for a bimolecular elementary reaction step:

$$A + B \rightarrow C + D$$

in which the rate of reaction is:

$$\frac{d[A]}{dt} = -k[A][B]$$

and k is expressed by:

$$k(T) = AT^{b}\exp(-\frac{E_a}{RT})$$

where A and b are constants and Ea is the activation energy. If the equivalence ratio, flow of the reactant, and temperature varies significantly in the flame, the access to kinetic rates is challenging. The idea for a basic estimation would be to have an homogeneous mixture of vaporized fuel, air, diluents and products at a controlled temperature all over the reactor volume to facilitate comparison of the product composition (emissions) with a zero-dimensional set of inputs (temperature, flow of air, equivalence ratio, dilution ratio, pressure) for a given fuel. The values experimentally obtained could now be compared to computer simulation results based on a chemical mechanism and the well-stirred reactor theory.

The reaction should be reaction rate limited. An ideal combustor would have its mixture immediately vaporized and mixed once it goes into the reactor volume. We are close from reaching this objective when using preheated fuel and then spraying it into a

vaporization chamber where it mixes with the air at an high temperature. Within an adequate delay between the spray and the injection, the liquid fuel totally vaporizes. Then the mixing into the combustor chamber is realized in jet stirred reactor through an important amount of small orifices creating some sonic jets, stirring the reactor vigorously. In a gas turbine system, the sonic condition is difficult to reach. Actually, the negative pressure gradients on the compressor liner wall due to a negative relative pressure lead to wall buckling. In effect, the liner is generally thin for weight reasons and the buckling limit is reached before the sonic regime.

Inlet and Reactor Temperature

The inlet temperature is a significant parameter for the stability of the reactor as well as the flame temperature or reactor temperature in a well-stirred system. Indeed, in a well-stirred reactor, the composition is homogeneous and so is the temperature. This is an ideal model; nevertheless, in reality it can depend on heat transfer calculations to predict the limitation in terms of wall cooling and heat losses. Indeed the higher the flame temperature, the higher the heat transfer rates and the better the cooling should be to maintain the material of the combustor at a reasonable temperature. Considering the benefits of higher temperature, the hotter the inlet mixture, the more stable will be the flame. However for an air/fuel mixture in an ideal well-stirred reactor, the increase in inlet temperature implies an increase in flame temperature. In theory, within a sufficient residence time, a well-stirred reactor reaches the adiabatic flame temperature. Considering the reaction as adiabatic and that chemical equilibrium reached, the entire heat release should raise the mixture to the adiabatic flame temperature. In Figure 5-1, the adiabatic flame temperature is plotted at constant pressure for CH4/O2/N2 mixture for different mixtures and inlet temperatures.

Calculations were done using Cantera, on a GRI3.0 mechanism with fixed enthalpy and pressure by B.Fond [1]. For a given oxygen-to-nitrogen ratio, the adiabatic flame temperature is maximum at a near stoichiometric mixture (O2/CH4=2). Indeed, the maximum heat of reaction per unit mass is obtained as almost all of the reactants are consumed to give CO2 and water. Therefore the flame temperature versus equivalence ratio curve is a bell whose top is near the stoichiometric point. The composition of the equilibrium mixture is shown on Figure 5-2. One can observe that for a stoichiometric mixture the products are essentially CO2 and H2O and N2, and so the heat of reaction is maximized.

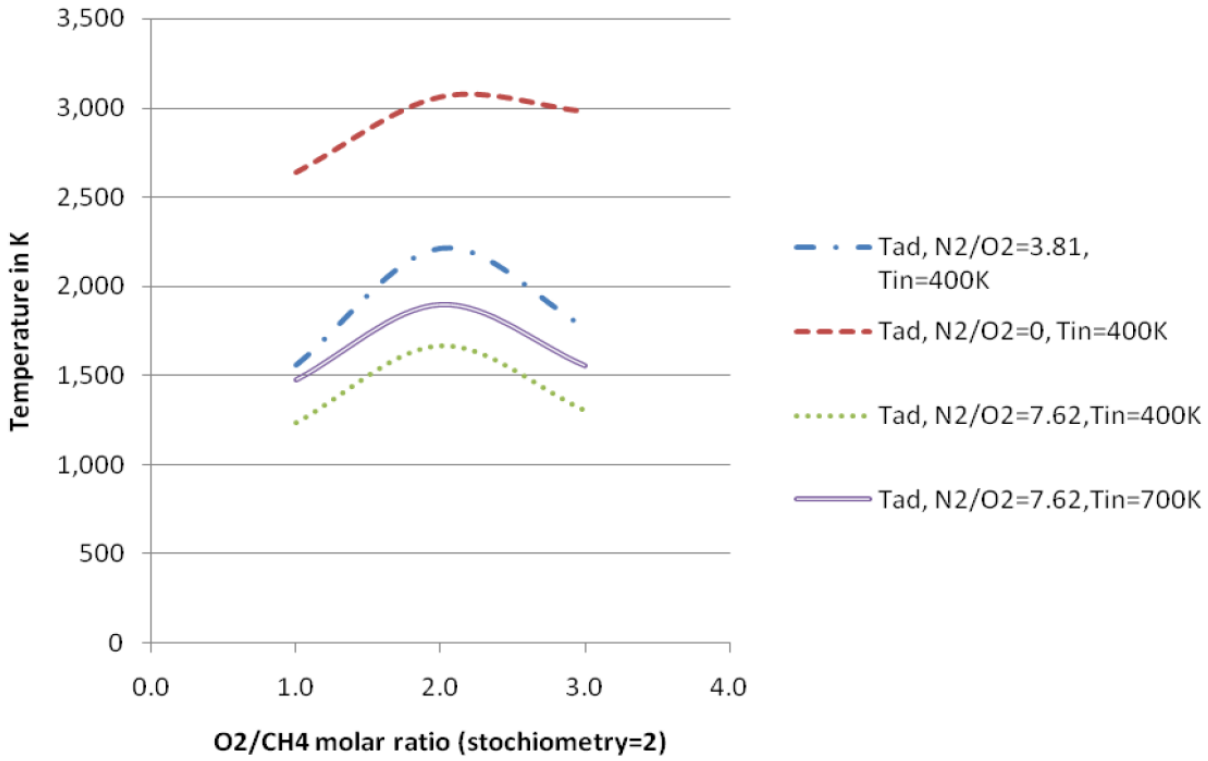

Figure 5-1. Adiabatic flame temperature for mixtures of CH4/O2/N2

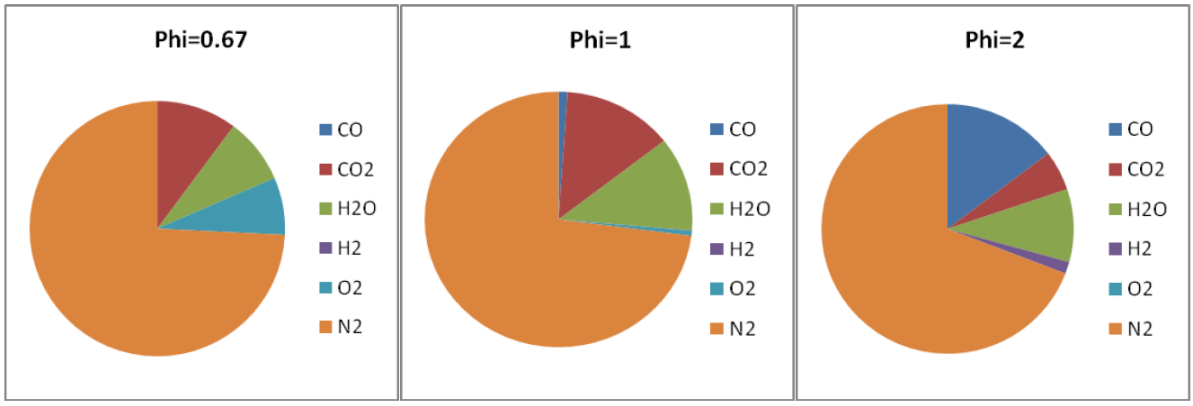

Figure 5-2. Composition at equilibrium for different methane-air mixtures at initial temperature of 400K and a constant pressure of 1 atmosphere

On the lean side, one sees that a good part of the oxygen remains in the products, and so the inert oxygen consumes some of the reaction enthalpy to reach the adiabatic flame temperature. As one goes toward rich mixtures, the concentration of CO which enthalpy of formation is lower than CO2 becomes predominant. For this reason, the combustion could be considered as incomplete as not all the CO is completely oxidized in CO2 following the reaction:

$$2CO + O_2 \rightarrow 2CO_2$$

The water-gas shift equilibrium is also involved on rich combustion leading to the formation of H2 in the products. The reaction involved is:

$$CO + H_2O \rightarrow CO_2 + 2H_2$$

Even though the mass fraction is low, the lightness of hydrogen hides a large molar fraction of 17.2%. As one goes toward a pure oxygen/fuel mixture, there is little or no inert species, and so less heat is needed to raise them to the final temperature, and therefore the remaining reacting species are heated to a higher temperature.

On the other side, as level of dilution by inert gases such as nitrogen is increased, the adiabatic temperature drops directly linked to the thermal effect of dilution. This type of combustion is of particular interest since the reactor is at a reasonable temperature and the gradient between the inlet temperature and the adiabatic flame temperature is fairly small promoting a homogeneous reaction zone. This is one of the ideas behind flameless combustion or moderate and intensive low oxygen diluted combustion. However the kinetic rates are very slow at 400K in a diluted regime, which could not be observed from adiabatic temperature results. Therefore, the flameless combustion concept is also called high temperature air combustion. The goal is to have a high inlet temperature with a small temperature rise due to combustion. This high inlet temperature is usually obtained by an exhaust gas recirculation as mentioned previously in this thesis. The hot exhaust gases are cooled down to 700-800K mix with the fresh air and are injected back into the combustion chamber. We maximize the heat extracted from the combustion but we lower the combustion chamber temperature. Most studies performed on well-stired reactor based their measurements on an air/fuel mixture inlet temperature of about 400K.

We can use our measurements of local temperatures inside the burner to build the burner's thermal map which includes temperatures and heat flux. In order to create this thermal model, we can split the whole burner into 6 distinguished areas: the inner cooling flow, the premixed gas/air flow, the outer flow, the inner tube, the outer tube and the rig case tube. These areas are shown on Figure 5-3.

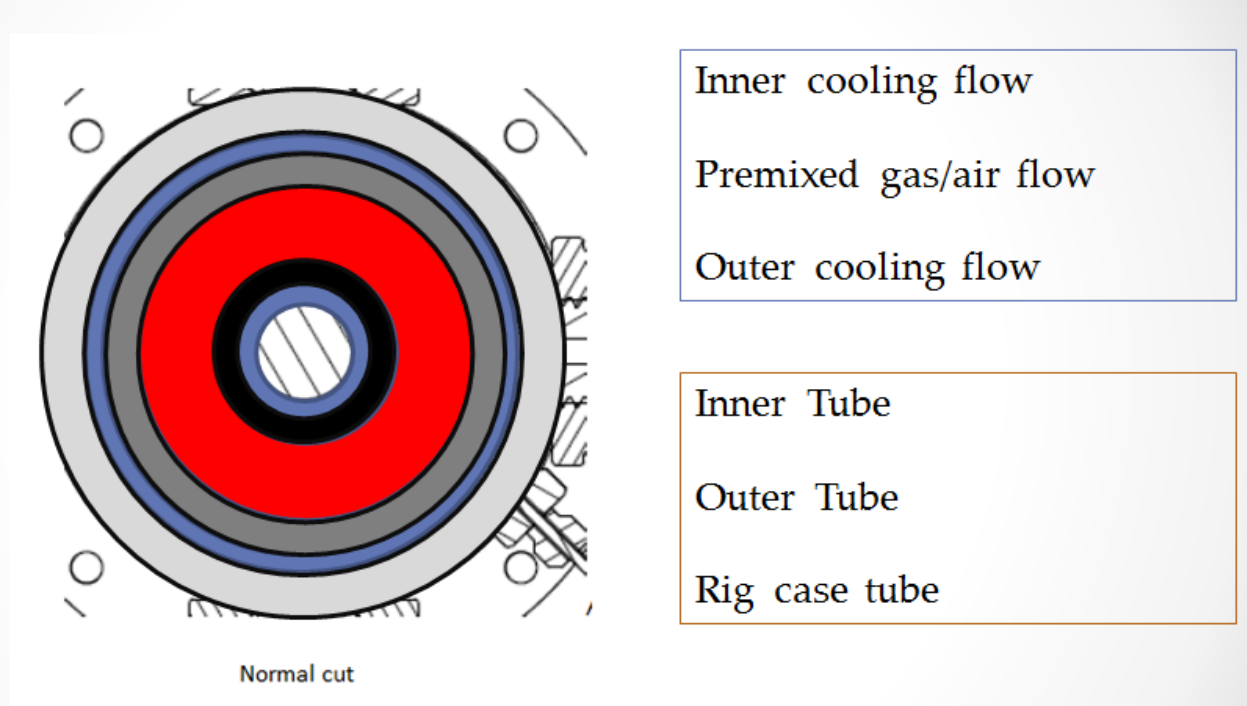

Figure 5-3. Schematic representation of the 3 flows and the 3 tubes of the burner's thermal modelisation

Experimental Feedback

It is interesting to compare the numerical investigation as shown Figure 5-2 with our experimentations results, to quantify the difference between those and to explain the main causes of our simulation's relative lack of precision. With our numerical investigation of the combustion performance of the reactor we obtained estimations of 0.5 and 1.75 for respectively the lean and the rich blowout ratios [1]. The investigation was performed using GRI 3.0 data and a Python/Cantera program. We experimentally obtained ratios of 0.68 and 1.63. The relative errors could then be estimated at 26% and 7% for respectively the lean and the rich blowout ratios.

These differences between experimentation and simulation results may come from the fact that the flame is not fixed with respect to the burner. Actually, the flame is transitioning when approaching blowout. Indeed, the flame is vertically translating inside the burner, positioning itself at the exit when running too rich and positioning itself at the

bottom of the annular space when running too lean. In addition to changing the blowout ratios, this transition phenomenon also impact the temperature measurement, since the thermocouples are not moving with respect to the burner. As we can see on the temperature graph Figure 4-1 and Figure 4-2 the “bell curves” are impacted by these phenomena. We could obtain the original curves by using an external observation system such as a camera system positioning the flame and using an expected temperature profile of the flame. We would then have more accurate temperature measurements.

In addition, we were not able to perform our experimentations under the exact same conditions as the ones assumed in our model. Indeed, since we were able to hear some combustion noises while carrying out the measurements, we can assume that the injected mixture was not entirely homogeneous. Without a doubt the noise of the flame was generated by local oscillations of the flame due to local non homogeneity in the flow composition. As mentioned in chapter 1, the well stirred reactor model considers uniform physical and thermo-chemical properties over the combustor.

These Observations give us some guidelines about future implementation around the whole operating system.

CHAPTER 6
FUTURE WORK

The implementation of this novel combustion system offers flexibility for parametric studies and constant developments. With the concrete implementations, the effect on the stability performance of very different parameters can be studied.

The characterization work of the rig could be completed using gas such as H2 and recomposed synthetic gas. As explained before, the gas supply lines have been implemented in a flexible way, allowing the injection of various mixtures in the burner. For example, injecting a preheated CO2-based mix could be used to simulate exit gases recirculation. Operating ranges of the burner should also be defined for every possible injector's orientation. This characterization studies should conclude on the identification of flameless combustion configurations for injected gas with different physical properties, thermo chemical properties and oxidation chemistry.

The same characterization work should be done with the liquid fuel injections. The main difference with gas is that these lines are preheated. Thus both air and fuel will be preheated. As mentioned in the "implementation" chapter, the temperature control box is controlling both the liquid fuel and injected air temperatures.

Using the gas analyzer available at the solar park, it would be relevant to profile the gas composition at the exit of the burner. This would help us to obtain sharper measurements of the CO2, CO and NOx density at the exit and give us a better idea of the efficiency of our reducing-NOx efforts.

Additionally, we should think about the implementation of a transverse nitrogen guided probe to perform real time sampling toward a GC-MS (Gas Chromatograph-

Mass spectrometer) or a SMPS (Scanning Mobility Particle Spectrometer). This would enable precise species analysis (GC-MS), and particle size distribution (SMPS).

Furthermore, we could think of implementing a microphone to record sounds coming from the burner. Indeed, having a measurement of the frequency and the intensity of the sounds coming from the burner would be very useful. B. Mühlbauer, R. Ewert, O. Kornow and B. Noll worked on Broadband combustion noise simulations [18]. They presented a numerical broadband combustion noise simulation of open non-premixed turbulent jet flames applying the Random Particle-Mesh for Combustion Noise (RPM-CN) approach. The RPM-CN approach is a hybrid Computational Fluid Dynamics/Computational Aeroacoustics method for the numerical simulation of turbulent combustion noise, based on a stochastic source reconstruction in the time domain. The combustion noise sources were modeled on the basis of statistical turbulence quantities, for example achieved by a Reynolds averaged Navier-Stokes (RANS) simulation, using the Random Particle-Mesh (RPM) method. RPM generates a statistically stationary fluctuating sound source that satisfies prescribed one- and twopoint statistics which implicitly specify the acoustic spectrum. Subsequently, the propagation of the combustion noise was computed by the numerical solution of the Linearized Euler Equations. Computed radial profiles of the reacting flow field were compared to experimental data and discussed.

The acoustic model used in their work is given by:

$$\frac{\partial \rho'}{\partial t} + u.\nabla\rho' + u'.\nabla\bar{\rho} + \bar{\rho}\,\nabla.u' + \rho'\nabla.u = 0$$

$$\frac{\partial u'}{\partial t} + (u.\nabla)u' + (u'.\nabla)u + \frac{\nabla p'}{\bar{\rho}} - \frac{\nabla\bar{p}\rho'}{\bar{\rho}^2} = 0$$

$$\frac{\partial p'}{\partial t} + u.\nabla p' + u'.\nabla \bar{p} + \gamma \bar{p}\ \nabla.u' + \gamma \rho' \nabla.u = q_p$$

With the combustion noise source term:

$$q_p = \frac{\overline{\gamma p}}{T}\frac{DT''}{Dt}$$

Where is the substantial time derivative:

$$\frac{D}{Dt} = \frac{\partial}{\partial t} + u.\nabla$$

A very similar study, using the same models could be done on our combustion rig. Finally, an advanced reactor model would be useful for understanding of the combustion behavior in the burner. Reacting turbulent flow simulations are a necessary step and analysis have to be performed with the purpose of choosing the best simulation in terms of computing time, complexity and predictions between different models. A good matching between the kinetic simulation and the experimental results will be essential to offer data on fuel oxidation kinetics.

APPENDIX A
RELEVANT MACHINING DRAWING

The drawings presented in this Appendix are not necessarily at the scale. The reader should refer to the dimensions noted on the drawings. Only relevant views to the understanding of the geometry are presented here. The complete geometry description of the burner is available in B.Fond's dissertation [1].

ASS-1 Axial assembly Cut

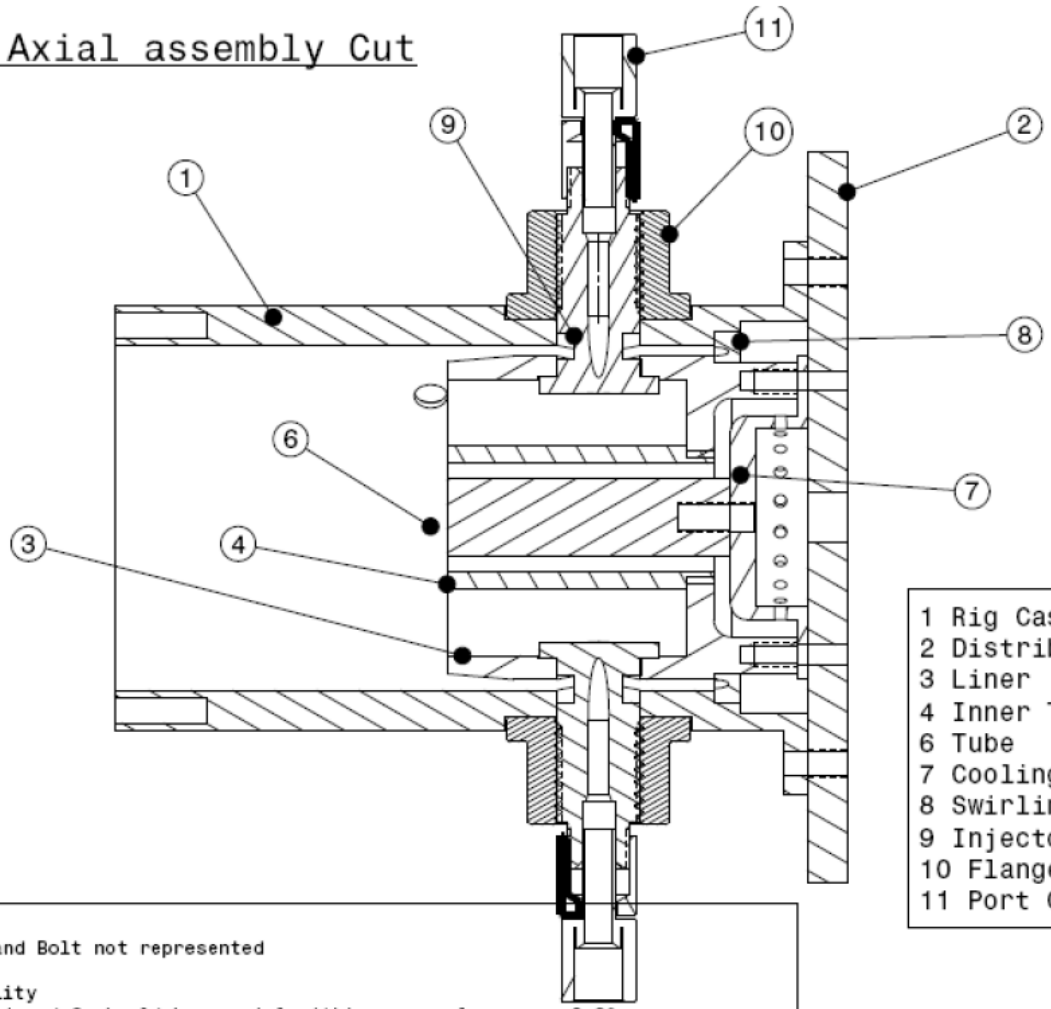

1 Rig Casing
2 Distribution Plate
3 Liner
4 Inner Tube
6 Tube
7 Cooling Liner
8 Swirling Vane
9 Injector (X4)
10 Flange lock (X4)
11 Port Connector (X4)

Note
Screw and Bolt not represented

Coaxiality
Pieces 1 and 3 should be coaxial within an angular error 0.2°
Pieces 4 and 6&7 assembled should be coaxial within an angular error of 0.2°

Tight Slide Fit between 8 & 1

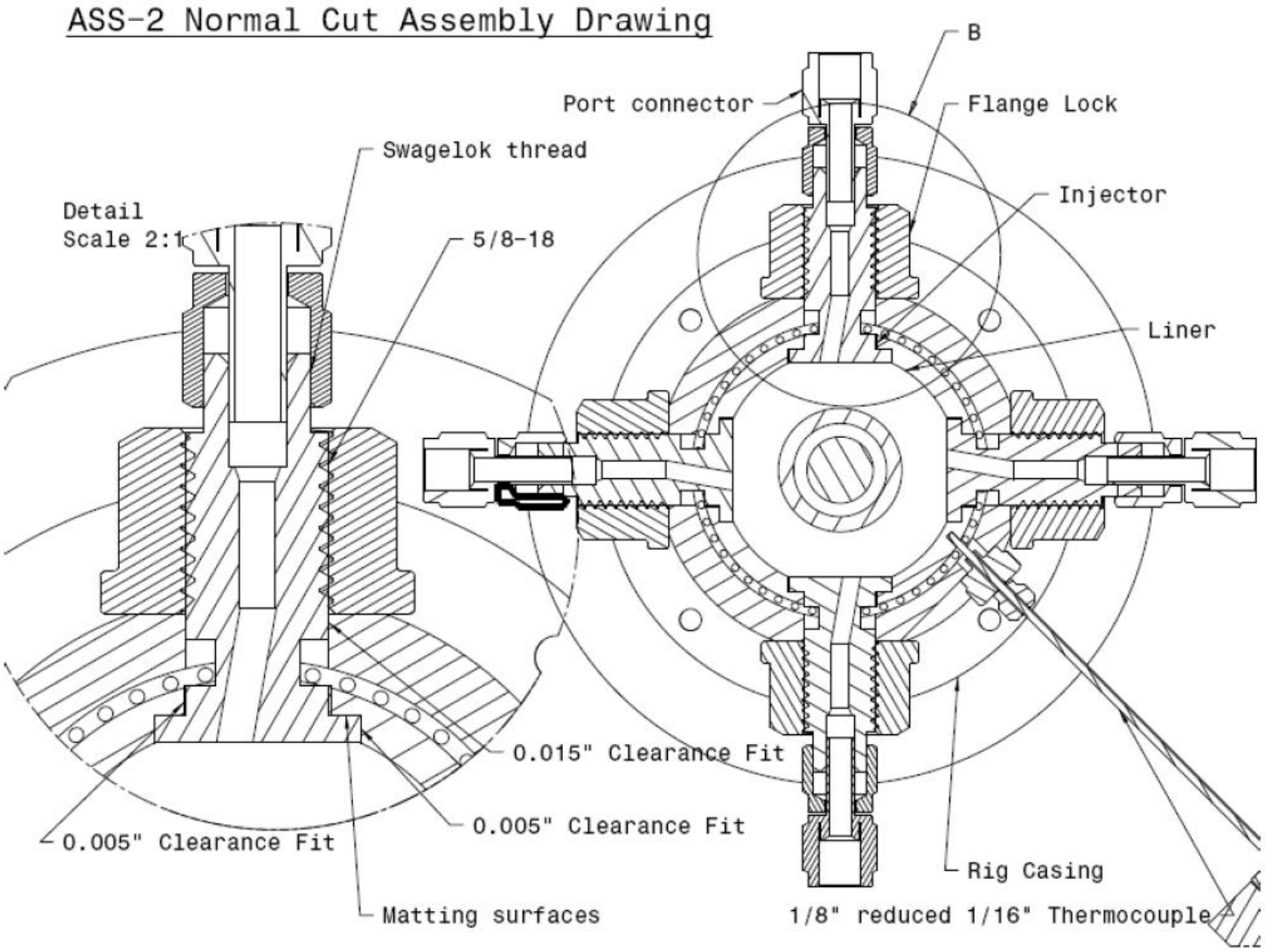
ASS-2 Normal Cut Assembly Drawing
B
Port connector
Flange Lock
Swagelok thread
Injector
Detail
Scale 2:1
5/8-18
Liner
0.015" Clearance Fit
0.005" Clearance Fit
0.005" Clearance Fit
Rig Casing
Matting surfaces
1/8" reduced 1/16" Thermocouple

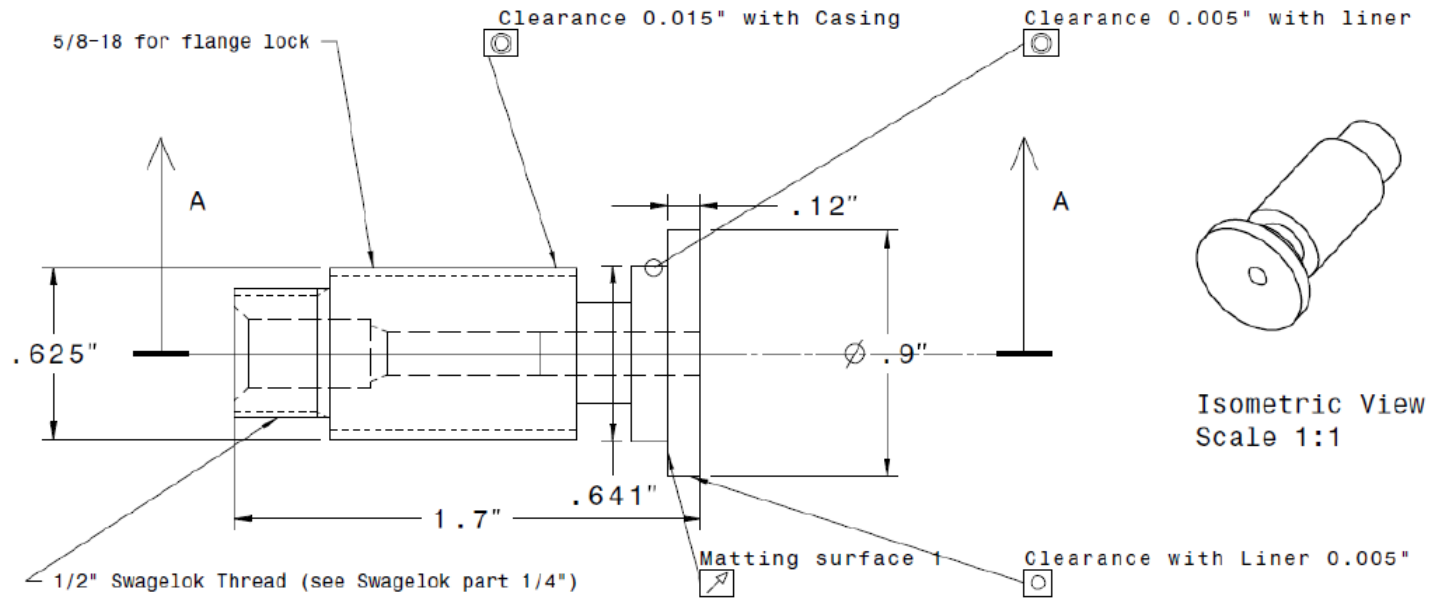

Isometric View
Scale 1:1

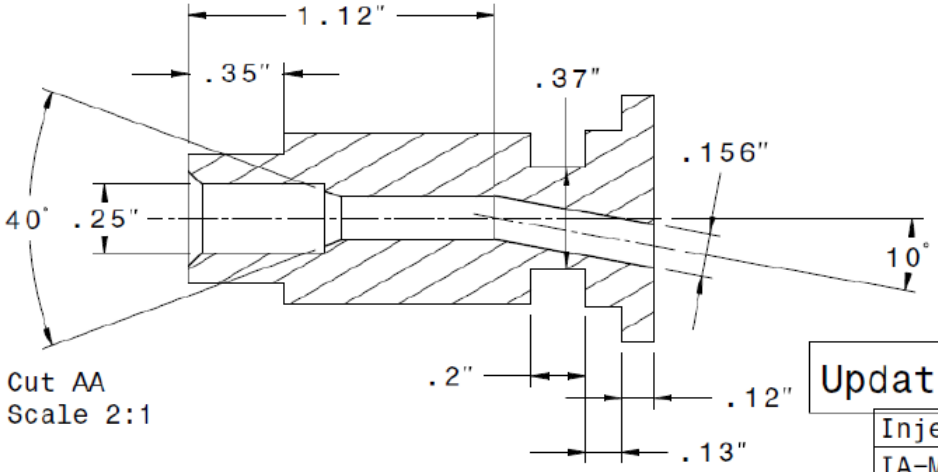

Cut AA
Scale 2:1

Note 1: Diameters could be adjusted to provide specified clearance given that specified 0.641" diam > max thread diam (0.625") +0.01" Clearance

Note 2: Left end of injector should correspond to provided Swagelok piece (conical hole and external thread)

Updated Version 4 09/20/09

Injector A	Hastelloy X
IA-M1.3-1	4 pieces

APPENDIX B
BIG PICTURE OF THE SUPPLY SYSTEM

A schematic plan representing the supply lines can be useful for the understanding of this thesis. The next page contains such a plan.

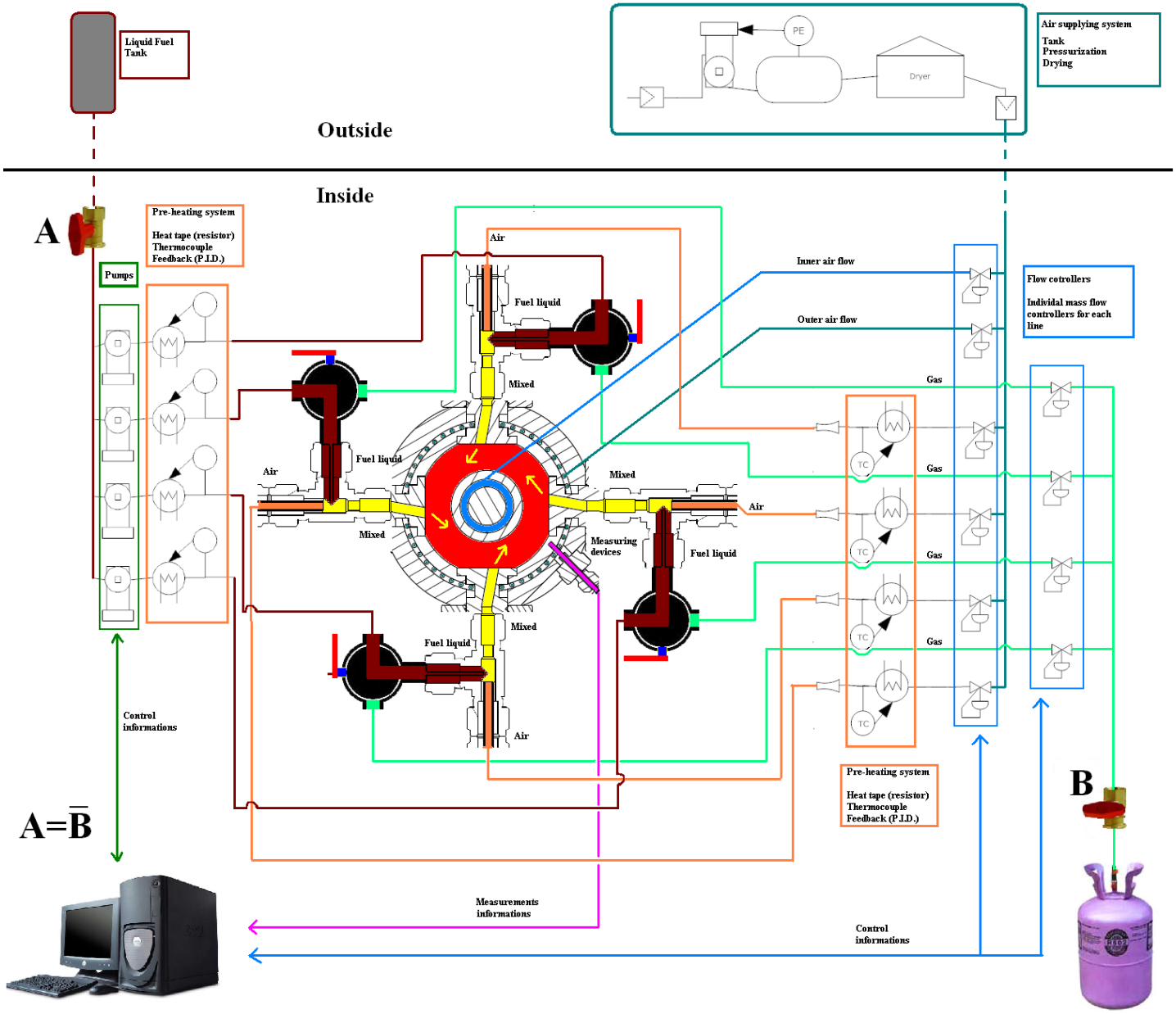
Liquid Fuel Tank
Outside
Air supplying system
Tank
Pressurization
Drying
PE
Dryer
Inside
A
Pre-heating system
Heat tape (resistor)
Thermocouple
Feedback (P.I.D.)
Pumps
Air
Fuel liquid
Mixed
Inner air flow
Outer air flow
Flow controllers
Individual mass flow controllers for each line
Gas
TC
Measuring devices
Control informations
A=B̄
Measurements informations
B

LIST OF REFERENCES

[1] B. Fond, Master Thesis, University of Florida, Gainesville, 2009.

[2] R. M. Heck, Catalysis Today 53 (1999) 519–523.

[3] J.A. Wunning, J.G. Wunning, Prog. Energy Combust. Sci., 23 (1997) 81–94.

[4] Zeldovich, J., The oxidation of nitrogen in combustion and explosions, Academy of Science of the USSR. Acta Physiochimica U.R.S.S., (1946), XXI(4).

[5] Ying Huang and Vigor Yang, Combustion and Flame 136 (2004) 383–389.

[6] Goy CJ, James SR, Rea S. Progress in Astronautics and Aeronautics (2005) 210:163–75.

[7] Ying Huang, Vigor Yang, Progress in Energy and Combustion Science, 35 (2009) 293–364.

[8] Alexander Stein, Saeid Niazi, and Lakshmi N. Sankar, Journal of Aircraft (2001) Vol. 38, No. 3.

[9] C. Dopazo, E. E. O'Brien, Acta Astronautica, (1974) Vol. 1, pp. 1239-1266.

[10] Z. ZhenLong, C. Zheng and C. ShiYi, Correlations for the ignition delay times of hydrogen/air mixtures, Peking University, Beijin, 2009.

[11] D. M. Kalitan, J.D Mertens, M.W. Crofton, E. L. Petersen, J. Propulsion and Power, 23 (2005) 1291.

[12] J. Natarajan, T. Lieuwen, J. Seitzman, Combust. Flame 151 (2007) 104–119.

[13] Q. Zhang, D. R. Noble, T. Lieuwen, Trans. ASME 129 (2007) 688-694.

[14] J. P. Longwell, M. A. Weiss, Indust. Eng. Chem. 47 (1955) 1634-1643.

[15] W. Tsang, S. Manzello, C. Stroud, M. Donovan, V. Babushok, K. Smyth, C. Frayne, D. Lehnert, S. McGivern, S. Stouffer, V. R. Katta, Kinetic Data Base for PAH Reaction and Soot Particle Inception during Combustion, SERDP Project WP-1198, 2007.

[16] Martin Skov Skjøth-Rasmussen, PhD dissertation, Technical University of Denmark, Kgs. Lyngby, 2003.

[17] Ian M. Kennedy, Prog. Energy Combust. Sci. (1997) Vol. 23, pp. 95-132.

[18] Helge Egsgaard, Investigation of the Initial Reactions of the Calcote Mechanism for Soot Formation, Riso National Laboratory, DK-4000 Roskilde, Denmark, 1996.

[19] Bernd Mühlbauer, Roland Ewert, Oliver Kornow and Berthold Noll, Aeroacoustics (2012) volume 11 number 1 pages 1-24.

BIOGRAPHICAL SKETCH

Julien Pierre-Michel Adrien Brissonneau was born in Mont Saint Aignan, France in 1989, the first of a three-child family. After two years of preparatory program in mathematics and physics at the Lycee Marie-Curie, he passed the entrance examination of Arts et Metiers Paristech where he pursued the 3-years *diplome d'ingenieur*. This degree is equivalent to a Master of Science in the French Graduate Schools of Engineering also called "Grandes ecoles". He studied mechanical and industrial engineering from 2008 to 2010 and enrolled at the University of Florida in August 2010 to pursue a Master of Science in mechanical engineering as part of a double diploma.